Interaction of acid mine drainage with biota in the Allchar Carlin-type As-Tl-Sb-Au deposit, Macedonia

Vladimir Bermanec[a], Ladislav A. Palinkaš[a], Željka Fiket[b,*], Jasna Hrenović[c], Anđelka Plenković-Moraj[c], Goran Kniewald[b], Ivan Boev[d], Blažo Boev[d]

[a] University of Zagreb, Faculty of Science, Department of Geology, Division of Mineralogy and Petrography, Horvatovac 95, 10 000 Zagreb, Croatia
[b] Institute Ruđer Bošković, Division for Marine and Environmental Research, Bijenička bb, 10 000 Zagreb, Croatia
[c] University of Zagreb, Faculty of Science, Department of Biology, Rooseveltov trg 6, 10 000 Zagreb, Croatia
[d] Goce Delčev University of Štip, Faculty of Natural and Technical Sciences, Blvd. Krste Misirkov, 10-A, P.O. Box 210, 2000 Štip, Macedonia

ABSTRACT

Allchar ore deposit, a well-known polymetallic mineralisation, is drained by the Majdanska River characterized by elevated concentrations of heavy metals and metalloids, particularly As, Tl and Sb. The present study was conducted at the spot of the confluence of spring water, heavily loaded with toxic metals, which joins the Majdanska River by a few meters short stream. The spring water is outflow of underground water drained by passage through polymetallic mineralisation. The chemical characteristics of the Majdanska River water and the associated periphyton were used to evaluate and explain the abiotic response to the intrusion of toxicants and its impact on biota.

At the site of the stream inflow, thorough mixing of Majdanska River water and incoming spring water resulted in an increase of Eh and pH close to the average river value. This geochemical barrier causes significant changes in the mobility of metal species. Moreover, the output composition of water is further modified by biological processes.

The examined biota community was found to consist of algae *Audouinella* sp. and *Spirogyra* sp., with coexisting freshwater snails *Radix labiata*, diatoms and bacteria.

While the carbonate bedrock controls the pH of the river water by effective buffering, it seems that bioconcentration and biomineralisation of algae exerted control on toxicants along the entire river flow. The highest bioconcentration factors were obtained for Fe, Mn and Ti which implies the biomineralisation of iron as a product of extracellular deposition on the cell walls on the organic matrices. Bioconcentration of As, Cr, Cs, Cu and Se was more important in *Audouinella* sp., while Cd, Co, Sr, and Zn preferentially accumulated in *Spirogyra* sp. High accumulation of Ba (3 mg/g d.w.) in *Spirogyra* sp. was associated with the intracellular biomineralisation. These findings suggest the potential use of *Spirogyra* sp. in the remediation of waters polluted by barium or as the biological pathfinder indicator for metal deposits associated with barite.

1. Introduction

Acid mine drainage (AMD) effects have created worldwide concerns for many years, largely over their negative impact on freshwater ecosystems, altering the diversity, structure, distribution and functioning of aquatic communities (Novis and Harding, 2007; Escarré et al., 2011; Bačeva et al., 2015; Talukdar et al., 2015; Nordstrom et al., 2015; Talukdar et al., 2017; Idaszkin et al., 2017). Remediation activities are currently being implemented at many sources of mine drainage with the goal of improving water quality in receiving streams. However, metal mining has increased at an alarming rate, and its residuals are not always treated adequately, often being released into small water bodies (Winterbourn et al., 2000; Doi et al., 2007).

Acid mine drainage affects the aquatic biota, benthic communities especially, by three main mechanisms – acidification, toxic concentrations of dissolved metals, and precipitation of metal hydroxides (mainly iron and aluminium hydroxides) (Nelson and Roline, 1996). Metal hydroxides and other metal compounds remain soluble at low pH but

precipitate at higher pH and can coat streambeds. As highly acidic waters increase in pH through buffering or dilution, a stage of precipitation and deposition of iron and then aluminium hydroxides will occur before the waters reach neutral pH. Although low pH and high concentrations of dissolved metals affect aquatic life, the deposition of metal hydroxides can result in more pronounced effects on the biomass of stream biota and ecological processes (He et al., 1997; Jakimska et al., 2011; Nordstrom et al., 2015). Failure to consider the role of precipitation of metal hydroxides can prevent successful prediction of ecological recovery in streams undergoing remediation.

To cope with environmental disturbances caused by AMD, a range of species evolved various physiological mechanisms to improve their tolerance to heavy metal toxicity (Baker et al., 1994). High tolerance to elevated levels of heavy metals was also reported for some freshwater algae (Goodyear and McNeill, 1999; Das et al., 2008; Rajfur et al., 2011; Chekroun and Baghour, 2013) and gastropods (Beeby and Eaves, 1983; Lau et al., 1996; Jordaens et al., 2006). These species have the ability to aggregate heavy metals within their organelles and are often used as bioindicators in polluted ecosystems (Goodyear and McNeill, 1999; Kaonga et al., 2008; Rajfur et al., 2010; Rajfur et al., 2011; Brayner et al., 2011; Durrieu et al., 2011; De Philippis et al., 2011; Mishra et al., 2011; Vogel et al., 2010; Kumar and Oommen, 2012). Algae (e.g. *Spirogyra* sp.) are also recognized as potential absorbents for heavy metals from mine or waste water (Gupta et al., 2001; Hamidian et al., 2013; Vetrivel et al., 2017).

The present study was conducted at the point of confluence of spring water which drains underground water of Allchar ore deposit and is heavily loaded with toxic metals, i.e. affected by AMD, with the Majdanska River. Flowing a fair part over carbonates, the Majdanska River, however, efficiently reduces acidity whereby toxicant concentrations are reduced to ecologically acceptable level. Thus, this site gives an opportunity to study geomicrobiological processes within this substantially polluted aquatic environment populated with algae and gastropods. The chemical characteristics of the Majdanska River water and associated periphyton, along with the data on present bacteria were used to evaluate and explain the abiotic response to the intrusion of toxicants and its impact on biota.

The effects of metal mining residuals in aquatic environments have already been reported for many areas in the world, including Europe (Rasmussen and Lindegaard, 1988) with impacts reported on fishes, invertebrates and macrophytes and even alterations in trophic webs, but data for south-eastern Europe is largely lacking.

1.1. Allchar ore deposit and short history of mining

The Allchar mine operated from 1881 to 1913 with some interruptions (Boev et al., 2001–2002). During this period mainly arsenic ore was excavated, with an estimated potential of 15,000 tons of arsenic (Ivanov, 1965). Exploration for antimony carried out from 1953 to 1957 and from 1962 to 1965 resulted in the discovery of significant reserves of low grade ore (Ivanov, 1986). Mineral potential of the Allchar deposit, both mined out and available ore, exceeds 20,000 tons of antimony with 0.5% Sb cut-off grade (Janković et al., 1997). In 1980s, thallium from the Allchar mine became of interest as a possible solar-neutrino detector (Freedman et al., 1976). It gave a new impulse to systematic exploration for the thallium commodity by the international LOREX project (LORendite EXperiment) (Ernst et al., 1984; El Goresy and Pavičević, 1988; Makovicky and Balić Žunić, 1993; and others). The mineral potential of thallium in the Allchar deposit has been estimated at 500 tons, and it is declared as the world-biggest thallium deposit, relative to reserves based exclusively on thallium minerals (Ivanov, 1986). During the 1986–1989 period gold mineralisation was also systematically explored. The results of both field and laboratory studies showed that the geological, geochemical, mineralogical and hydrothermal alteration features are similar to those which characterize Carlin-type mineralisation of the western United States (Stafilov and

Todorovski, 1987; Percival and Boev, 1990; Percival and Radtke, 1994; Strmić Palinkaš et al., 2018).

The Allchar mine, besides hosting common metal sulphides such as pyrite, marcasite, stibnite, realgar-orpiment-lorandite and their secondary equivalents, is a "garden" of thallium and arsenic sulphide and sulphosalts, like arsenopyrite $FeAsS$, bernardite $Tl(AsSb)_5S_8$, jankovicite $Tl_5S_9(AsSb)_4S_{22}$, lorandite $TlAsS_2$, parapierrotite $Tl(Sb,As)_5S_8$, picotpaulite $TlFe_2S_3$, dorallcharite $Tl_{0.8}K_{0.2}Fe_3(SO_4)_2(OH)_6$, raguiniteTlFeS_2, rebulite $Tl_5Sb_5As_8S_{22}$, simonite $TlHgAs_3S_6$, vrbaite $Tl_4Hg_3As_8Sb_2S_{20}$, weissbergite $TlSbS_2$, fangite Tl_3AsS_4, and an unnamed new mineral $Fe_2Tl[(As_{0.85}S_{0.15})O_4]_3 \cdot 4H_2O$. The ore body in the richest zone contains about 18,000 cubic meters of ore with an average Tl content of 0.35% (Boev et al., 2001–2002). The sulphide minerals typically compose > 10 and up to 50 vol% of the host rock (Strmić Palinkaš et al., 2018).

Although mining activities ceased in 1913, the adverse effects on the environment still persist. The operation of the mine released waste products, among which the highly toxic As and Tl, fortunately into a scarcely populated area. Apart from human activity (mining), natural exposure of the ore deposit to oxidation by intrusion of water and oxygen and dispersion of primary metal accumulation are a consequence of erosional processes. These started soon after the last deglaciation with high erosional rates from several tens m/Ma to 165 m/Ma, as determined by ^{26}Al, ^{36}Cl, and ^{21}Ne isotopic studies (Pavičević et al., 2016). The lower and upper limits of the paleo-depths for the ore body sector Centralni Deo are 250–290 and 750–790 m in the last 4.3 Ma, respectively. The upper limit of the paleo-depth for the ore body Crven Dol is 860 m over the same geological age (Pavičević et al., 2016).

2. Materials and methods

2.1. Site description

The Allchar ore deposit is located in the north-western region of Kožuf Mts. in the Republic of Macedonia (Fig. 1a, b). Nonetheless, the influence of mineralisation is notable in the wider area. The Majdanska River sediments contain elevated levels of antimony, likely an artefact of mining activities in the former Ottoman Empire (Bačeva et al., 2014). However, Bačeva et al. (2014) showed that the anthropogenic influence of the mine in the Allchar area was limited and had almost no impact on the distribution of As, Sb and Tl in the river sediments, except in the immediate vicinity of the former mine (Sb). The distribution of these elements in local soils and river sediments is related almost exclusively to the decomposition of mineralised rocks and subsequent pedogenetic processes (Bačeva et al., 2014). Moreover, the content of Tl in the close vicinity of Allchar area represents the highest established natural and anthropogenic augmentation of thallium in soil worldwide (Bačeva et al., 2014).

Although the surrounding of the Allchar mine is mostly uninhabited, the geochemistry of this area has been extensively studied (Lepitkova et al., 2013; I. Boev et al., 2014; B. Boev et al., 2014), due to possible adverse influences on agriculture. Namely, sediments from the Majdanska River are transported to the Crna River and deposited in its alluvial sediments, an area of intensive agriculture (Bačeva et al., 2014).

Near the study area, there is also Ržanovo mine (Fig. 1b), a deposit of Fe-Ni lateritic ore formed by laterization processes of ultrabasic complexes during the Upper Cretaceous (Serafimovski et al., 2012).

2.2. Geological and hydrogeological setting

Allchar is polymetallic Sb-As-Tl-Au deposit situated in the western part of the Vardar zone. It is spatially and temporally associated with Pliocene (~5 Ma) post-collisional high-K calc-alkaline to shoshonitic volcano-plutonic centre (Boev et al., 2001–2002). The deposit owes its
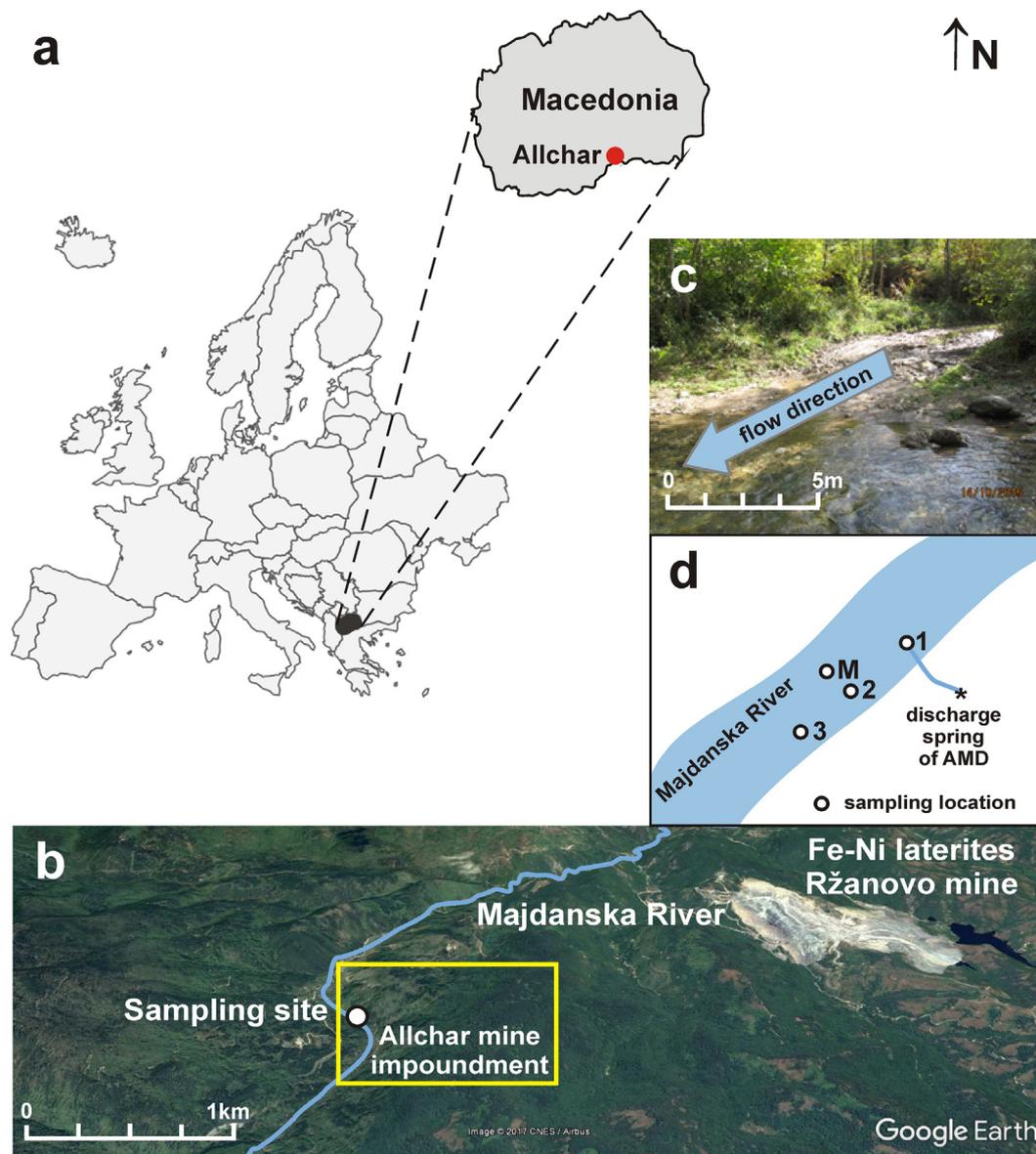
Fig. 1. Map of the study area, its geographical position (a), location of the Allchar mine and the Majdanska River (b), detailed view of sampling site (c) with indicated sampling locations (d).

complex lithology and tectonic structure to adherence of the unstable Vardar zone with Neotethyan geological heritage and rigid crystalline Pelagonian block (Boev and Serafimovski, 1996) (Fig. 2). The mineralisation is associated with the Pliocene volcano-intrusive complex of calc-alkaline suites (3.9–5.1 Ma, Janković et al., 1997), controlled by intersection of deep fractures striking mostly N-S and neotectonic ruptures with SW-NE directions. This igneous complex formed on a basement composed of Triassic sediments, Jurassic ophiolite (gabbro-peridotites prevail) and Cretaceous sediments. The host rocks of the mineralisation are predominantly carbonates of Triassic and Tertiary age, including some Pliocene-age tuffaceous and volcanoclastic sediments. This heterogeneous collage is highly hydrothermally altered by silification, argillitization, dedolomitization, sulphidation and supergene alteration typical of a humid climate. Pyrite and marcasite are replaced by Fe oxides and hydroxides, As-, Sb- and Tl-sulphides form oxides and oxysalts, and igneous and sedimentary rocks are converted to mixtures of secondary clay minerals.

The ore complex is highly porous and permissive to intrusion of meteoric waters and represents a rich aquifer containing acid mine drainage (AMD) as a carrier of toxic metals to the springs. The footwall

of the ore complex forms an aquitard incapable of transmitting significant amounts of spring water under prevailing hydraulic gradients. This barrier is partly composed of Precambrian gneisses and marbles that are conformably overlain by Paleozoic metasedimentary rocks, mostly phyllites, schists, metasandstones and marbles, forming the underlying complex of the Kožuf Massif.

The Allchar ore deposit at the flanks of the Kožuf Massif (Voras Massif in Greece) receives more annual precipitation (annual mean 800–1000 mm/y) than the wider area of Eastern Macedonia (600–800 mm/y). The mine impounds are drained by the perennial stream of the Majdanska River, a tributary of the Crna River, a short "gaining stream flow" recharged by overflow, interflow and base flow with copious amounts of water. The saturation zone is above the elevation of surface water for most of the year (Fig. 3a). The conditions of "losing stream flow" (Fig. 3b) occur during the winter period when precipitation falls below 200–300 mm/y. Nonetheless, strong winter and spring precipitation, or ephemeral summer storms exert a large influence on the position of the water table and nature of the "base flow".

Favourable hydrological regime and carbonate bedrocks provide
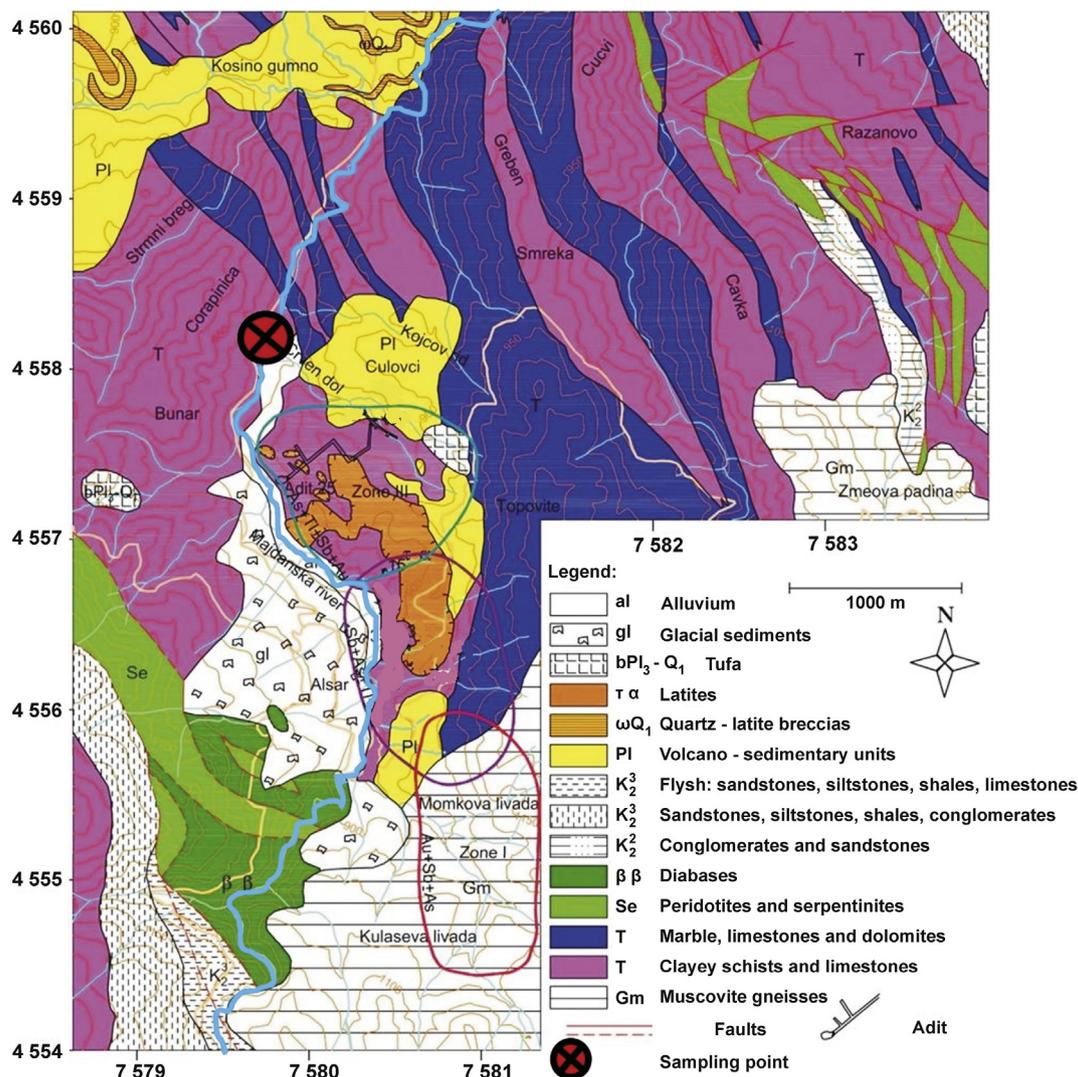
Fig. 2. Geological map (ref) of studied area (with indicated sampling point) shows complex geological environment (Janković et al., 1997).

requisite acidity buffering; however, contaminant concentrations remain above the permissible values. Dolomites, less affected by alteration processes or tectonic fracturing, behave as traditional karst aquifers with a base flow confined by a fault system. The result is discharge of polluted stream water above or below water surface, respectively. The heavily polluted groundwater is discharged into the Majdanska River by a "discharge spring", as termed further on in the text. Its character and interaction with river water and biota are the subject of this study.

2.3. Sample collection

Sampling was carried out in the Majdanska River (Fig. 1), at the crossing of the river and the dirt road to *Crven Dol* (GPS E 21°56′43.346″, N 41°9′51.084″). This crossing is characterized with a small spring and samples were collected at three locations, at the site of discharge of this spring into the Majdanska River (location 1) and downstream of discharge (locations 2 and 3) (Fig. 1c, d). At all locations, the depth of water was < 0.5 m. Samples were collected
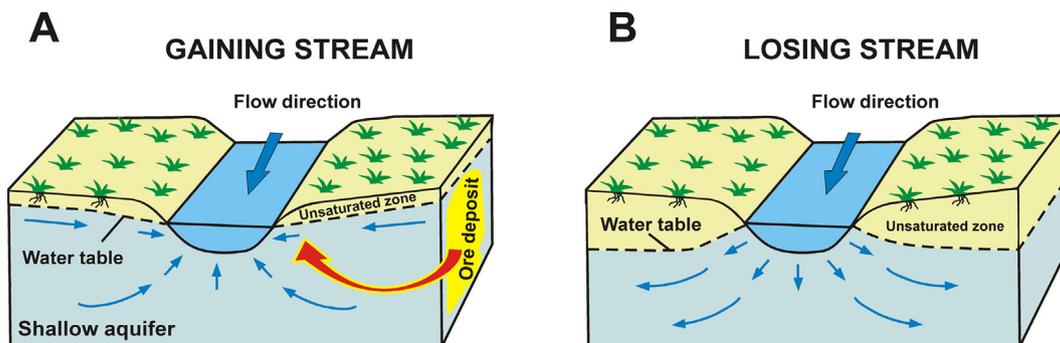

Fig. 3. Components of a river hydrography (after Maidment, 1992, slightly modified). The model depicts discharge of acid mine water into the Majdanska River.

following the recommendation on sampling methodology of European Commission (2000). Sampling was conducted in spring 2016, under "gaining stream flow" conditions.

A total of eleven water samples were collected at locations 1–3: three samples at the first site, four at the second and four at the third. Additionally, water (M) was sampled in the middle of the river, as shown in Fig. 1d. At each location, water samples were taken at a distance < 5 m in the following manner: 1) for bacteriological analyses, the samples were aseptically taken in sterile 1 L glass bottles and processed in the laboratory within 24 h after collection; 2) for trace element analysis samples were collected in glass bottles and immediately after sampling acidified with nitric acid, 1% *suprapur* HNO$_3$ (v/v). At each sampling location the sediment and periphyton were also collected, along with snails. Sediment (ca 0.5 kg) was sampled with a plastic sampling shovel and stored in a plastic bag. Samples of periphyton comprised of two macroscopically different communities and were collected by gently removing the stones from the water. Total of 4 snails, with an average size of 12–20 × 7–13 mm, was isolated from the algal biofilms. All samples were stored at 4 °C until further processing.

2.4. Sample preparation

The algal biofilms from the stones surfaces were scraped by brush into a dark specimen container and stored at −40 °C. Before storage, the samples were divided into subsamples for further analyses (biota assemblages, scanning electron microscopy (SEM) and multielement analysis), as described below.

For taxa identification, clusters of soft algae were repeatedly washed eight times with distilled water to remove the present epiphytes (diatoms). Subsamples of soft algae were preserved with 2% formaldehyde (final concentration). Cleaned diatom frustules subsamples were prepared following procedure described by Hendey (1964). Firstly, diatom subsamples were treated with hydrochloric acid (HCl) to remove calcium carbonate, and then the organic matter was removed with sulphuric acid (H$_2$SO$_4$) and sodium nitrate (NaNO$_3$). For SEM analysis, the soft algae and diatom subsamples were dehydrated in increasing series of ethanol aqueous solutions, dried on a critical point table-top dryer and then sputter-coated with gold.

Samples of water, periphyton (soft algae) and freshwater snail were subjected to multielement analysis. For that purpose, subsamples of soft algae were dried at 105 °C, lyophilized (Alpha 1–2, Christ, Germany) and homogenised using an agate mill. The snail soft tissue was removed from the shells with a plastic knife, air-dried and homogenised using an agate mill.

Prior to multielement analysis, subsamples (0.1 g) of algae and freshwater snail shell and tissue were subjected to a digestion in the microwave oven (Multiwave 3000, Anton Paar, Graz, Austria) with 7 mL of HNO$_3$ and 0.1 mL of HF (Filipović Marijić and Raspor, 2012). Sample digests were prepared for analysis by addition of indium (In, 1 μg L^{-1}) as internal standard, without further dilution.

Prior to analysis, aliquots of water samples were acidified with 2% (v/v) HNO$_3$ (65%, supra pur, Fluka, Steinheim, Switzerland) and indium (In, 1 μg L^{-1}) was added as internal standard.

Water, sediment and freshwater snail samples were also used for bacteriological analysis. For that purpose, samples were concentrated on the sterile membrane filters of pore size 0.45 μm in triplicate both before and after dilution in sterile peptone water.

2.5. Physico-chemical and trace element analyses

The physico-chemical parameters of the river water (pH, Eh, conductivity and dissolved oxygen) were measured in situ at all three locations (1, 2 and 3) according to the Standard Methods for Examination of Water and Wastewater (APHA, AWWA, WEF, 2005) by using a multiparameter portable set (Hach). The pH, Eh and conductivity were calibrated with standard solutions, with a precision of 0.01 pH unit,

1 mV and 1 μS/cm, respectively, while the oxygen probe (accuracy of 0.01 mg/L) has an automatic internal calibration. The multielement analysis of water, algae and snail shell and tissue samples was performed by High Resolution Inductively Coupled Plasma Mass Spectrometry (HR-ICP-MS) using an Element 2 instrument (Thermo, Bremen, Germany). Typical instrument conditions and measurement parameters used throughout the work were reported earlier (Fiket et al., 2007, 2017).

All samples were analysed for total concentration of 25 elements (Ag, Al, As, Ba, Be, Bi, Cd, Co, Cr, Cs, Cu, Fe, Li, Mn, Mo, Ni, Pb, Rb, Sb, Se, Sr, Ti, U, V and Zn). Quality control of analytical procedure was performed by simultaneous analysis of the blank and certified reference material for water (SLRS-4, NRC, Canada) and Rye grass (ERM 281, IRM, Belgium). A good agreement between the analysed and certified concentrations within their analytical uncertainties for all elements was obtained (± 10%).

2.6. Analysis of periphyton

Taxa were identified to species level where possible and counted at 1000× magnification using an Olympus BX-51 microscope equipped with a 100× phase contrast objective (numerical aperture: 1.25).

For the determination of algal species, recent taxonomic literature was used (Hindák et al., 1978; John et al., 2002; Krammer, 2002; Krammer and Lange-Bertalot, 1991a, 1991b; Lange-Bertalot, 2001; Lange-Bertalot and Genkal, 1999; Patrick and Reimer, 1975; Round et al., 1990; Wehr and Sheath, 2003).

Diatoms were examined under Gemini Supra Carl Zeiss scanning electron microscope (EHT = 1.00 mV, WD from 2.9 to 3.4 mm) in the Laboratory for electron microscopy and microanalyses at the University of Pretoria. The abundance of established diatoms was expressed as percentage of occurrence frequency for each species. In order to relate the diatom community to water quality, Saprobic Index SI (Wegl, 1983) and Trophic Diatom Index TDI (Rott et al., 1999), were calculated.

2.7. Bacteriological analysis

Aerobically grown total heterotrophic bacteria were determined on Nutrient agar (Biolife) after incubation at 22 °C/72 h (APHA, AWWA, WEF, 2005). Carbapenem-resistant bacteria were determined on CHROMagar Acinetobacter supplemented with CR102 (CHROMagar), which allows the growth of carbapenem-resistant bacteria (Hrenović et al., 2016) after incubation at 37 °C/72 h.

The numbers of aerobically grown total heterotrophic bacteria and carbapenem-resistant bacteria were determined as Colony Forming Units (CFU), logarithmically transformed, and expressed as log CFU per 1 mL of water or 1 g of sediment and freshwater snail.

Statistical analyses were carried out using Statistica software 12 (StatSoft, Inc.). Absolute numbers of bacteria were logarithmically transformed. The comparisons between variables were done using the ordinary Student's *t*-test for independent variables. Statistical decisions were made at a significance level of p < 0.05.

2.8. Basic prediction for the destiny of toxicants in the Majdanska River

Monovalent cations, Li$^+$, Rb$^+$, Cs$^+$, and divalent Sr^{2+}, act as conservative ions in aqueous media, showing dilution effects without changes in speciation under near neutral conditions. They can be regarded as pH non-specific during adsorption on hydrous iron oxides (Musić and Ristić, 1988).

On the other hand, divalent cations, e.g. Ba^{2+}, Be^{2+}, Cd^{2+}, Co^{2+}, Cu^{2+}, Ni^{2+}, Pb^{2+} and Zn^{2+}, become increasingly insoluble as the pH increases (Evangelou, 1998; Gaillardet et al., 2003). At the near-neutral pH, the solubility of the most heavy-metal cations is severely limited by precipitation/co-precipitation with Fe-Ti-Al-Mn oxides and hydroxides, or, which is more likely, by their strong adsorption on aforementioned

hydrous metal oxides due to ongoing deprotonation processes (Gaillardet et al., 2003; Szekeres and Tombácz, 2012).

Elements such as bismuth, chromium and vanadium, readily form oxo-complexes in aqueous media. Bismuth is stable as oxo-complex $Bi_6O_6^{6+}$ at low pH values (Brookins, 1988), while under normal surface conditions of Eh and pH Bi^{3+} is rapidly hydrolysed and tends to form insoluble basic salts. Chromium easily changes valence states from Cr^{6+} to Cr^{3+} and vice versa (Tingzong et al., 1997). Redox boundary between reduced and oxidised forms depends on Eh and pH. Oxyanion CrO_4^{2-} is mobile and highly toxic form, readily reduced by Fe^{2+} to Cr^{3+} which hydrolyses as $Cr(OH)^{2+}$, $Cr(OH)^+$ and $Cr(OH)_3$ behaving as other trivalent cations and co-precipitating with iron hydroxide. Manganese (MnO_2) catalyses oxidation of Cr(III) species, which releases chromium by its most toxic form (Tingzong et al., 1997).

Vanadium valences range from 2^+, 3^+, 4^+ and 5^+. Their representatives are soluble over the broad Eh-pH range. Vanadium (IV) at lower pH forms vanadyl ion (VO^{2+}), while vanadium (V) forms an extensive family of oxyanions (Brookins, 1988; Gaillardet et al., 2003). Orthovanadate ion VO_4^{3-} is the principal species present at pH 12–14. On the other hand, protonated vanadates, $H_2VO_4^-$, HVO_4^{2-} are dominant at lower pH. Uranium, selenium and arsenic change their valence state under variable redox conditions giving way to a plethora of mobilising and immobilising forms in near-surface environment. Under oxidising conditions, these elements form stable positive and negative ion complexes in their higher valences. As the pH increases, most oxyanions tend to become less strongly adsorbed, even at neutral values (Dzombak and Morel, 1990). The oxyanion-forming elements such as As and Se as well as uranyl-carbonate complexes show high mobility not constrained by adsorption effects. Their negative charge stays in repulsive relation with deprotonised surfaces of colloids (Gaillardet et al., 2003; Szekeres and Tombácz, 2012).

In the Allchar deposit, the arsenic is present as the major element in the form of realgar and arsenopyrite minerals. There is a long list of As-Tl-Sb-Fe minerals which contribute to arsenic and thallium species by weathering of ores and mine waste dumps. Redox potential (Eh) and pH are the most important factors controlling arsenic speciation. Under oxidising conditions, $H_2AsO_4^-$ is dominant at low pH (less than about pH 6.9), while at higher pH, $HAsO_4^{2-}$ becomes dominant ($H_3AsO_4^0$ and AsO_4^{3-} may be present in extremely acidic and alkaline conditions, respectively). Under reducing conditions, at pH < 9.2, the uncharged arsenite species $H_3AsO_3^0$ will predominate (Brookins, 1988).

Oxidation of arsenic minerals in the ore deposit impoundment competes for O_2 with oxidation of pyrite. The pyrite can undergo oxidation by two natural oxidants, oxygen and even more effective ferric (Fe^{3+}) ion according to simplified reactions such as:

$$FeS_2 + 3.5O_2 + H_2O = Fe^{2+} + 2SO_4^{2-} + 2H^+$$

$$FeS_2 + 14Fe^{3+} + 8H_2O = 15Fe^{2+} + 2SO_4^{2-} + 16H^+$$
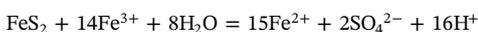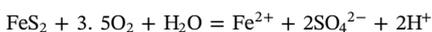
These two reactions bring about a considerable decrease in pH and an increase in concentrations of ferrous (Fe^{2+}) and sulphate ions in water (Migaszewski et al., 2007). High concentration of Fe and low pH (2.3) in an adit of the mine were evidenced by Alderton et al. (2005) (Table 1). Thus, predicted high concentrations of sulphate ions, and possibly phosphates (originating from apatite; Strmić Palinkaš et al., 2018), inhibit arsenic precipitation occupying colloid surfaces (Gaillardet et al., 2003; Szekeres and Tombácz, 2012). This constrains reducing conditions which define the As(V)/As(III) ratio. This ratio undergoes significant change by discharge of mine water into the Majdanska River, but its quantitative outcome is ambiguous, due to slow kinetics of arsenate-arsenite oxidation (Tallman and Shaikh, 1980).

Thallium exists in three valence states, +1, +2, and +3, but only monovalent Tl(I) and trivalent Tl(III) are present in nature. Their toxicity depends on the oxidation state, and Tl(III) is 50,000 more toxic than the Tl(I) (Karbowska, 2016). However, according to Tremel et al. (1997) monovalent thallous cation occurs in natural waters almost exclusively. Namely, thallium (III) has an exceptionally strong oxidation potential and is readily reduced into Tl(I), which explains its subordinate presence in natural compartments (Brookins, 1986).

3. Results and discussion

3.1. Water quality data

The measured physico-chemical parameters (pH, Eh, conductivity, and dissolved oxygen) displayed low variability between sampling points. Their average values are given in Table 1. The mean pH value characterises water of the Majdanska River as slightly alkaline, while the Eh falls in the range characteristic of freshwater systems. The pH, conductivity and dissolved oxygen values coincide with values generally attributed to conditions supporting diverse aquatic life, and suspended solids indicate high water clarity of the Majdanska River water.

3.2. Species composition

The two macroscopically different periphyton communities observed in the field were identified as *Audouinella* sp. Boryand and *Spirogyra* sp. Link (Fig. 4). Among the diatom assemblages 12 species were established with predominance of Cocconeis and Gomphonema group (Fig. 5, Table 2).

Algae are significant indicators for the environmental quality of aquatic ecosystems (Hering et al., 2006; Chen et al., 2008; Kelly et al., 2008). Due to widespread distribution, their small size and very short generation time (Stevenson and Pan, 1999), they are the main primary producers well established in aquatic food webs and are very sensitive to majority of physicochemical and ecological changes in the environment. Calculated TDI and SI values range from 2.0 to 3.2 and 1.8 to 2.8, respectively, indicating good environmental status in terms of water quality.

The freshwater snails, identified as *Radix labiate* (Rossmässler, 1835–1837), were found inside of both identified algal communities, probably feeding on them. Sporadically, some bacteria were also found in association with identified algae. The most abundant rod-shaped form was observed on the soft algae surfaces (Fig. 6).

3.3. Trace element distribution in water and biota

Results of measurement of 25 elements (Ag, Al, As, Ba, Be, Bi, Cd, Co, Cr, Cs, Cu, Fe, Li, Mn, Mo, Ni, Pb, Rb, Sb, Se, Sr, Ti, U, V and Zn) in water, soft algae communities and snail shell and tissue samples are shown in Table 1. For comparison, the concentrations reported by FOREGS for the nearby area (Salminen et al., 2005), data for thermal waters from Kožuf mountain (Boev and Jančev, 2014) and the Majdanska River (upstream from mineralisation; Alderton et al., 2005), as well as those reported for standing water in an adit in Allshar (Alderton et al., 2005) were added to Table 1.

The water samples 2, 3, and M displayed similarities regarding the level of measured elements. The highest concentrations were obtained for As (99.8–145 µg L^{-1}), Fe (31.7–67.3 µg L^{-1}) and Sr (127–167 µg L^{-1}), while the lowest concentrations were observed for Bi (0.002–0.004 µg L^{-1}), Cd (0.008–0.030 µg L^{-1}) and Be (0.020–0.032 µg L^{-1}) (Table 1).

Since the Geochemical atlas of Europe (FOREGS, Salminen et al., 2005) lacks information on element concentration for Macedonian stream waters, the obtained results were compared to data for nearby Greek streams (Table 1). Namely, the Allchar deposit is situated close to the border of Republic of Macedonia and Greece, and the data available for nearby Greek streams are considered to mirror the water geochemistry determined by the geological background of the wider area, at the same time allowing for differentiation of elevated element

Table 1

Physico-chemical parameters (measured in situ at three locations) and mean values of element concentrations in water (µg L^{-1} or *mg/ L), algae (µg g^{-1}) and snail (µg g^{-1}) samples of the Majdanska River.

	Water								Algae		Freshwater snail			
	1	2	3	M	GR[a]	ThW[b]	A2[c]	A4[c]	*Audouinella* sp.	*Spirogyra* sp.	Shell A	Shell B	Tissue A	Tissue B
pH	7.62	7.76	7.80				7.6	2.3						
Eh [V]	0.183	0.167	0.170											
Cond. [µS/cm]	163.3	167.1	168.8											
S*							7.1	19,688						
O₂ [mg/L]	9.14	9.20	9.46											
Ag	3.05	0.038	0.066	0.082		< 2	0.1	0.2	0.239	0.131	0.199	0.091	0.681	0.241
Al	3619	42.0	23.1	34.5	6.50–9.50	2–67	0.0	2,040,000	902	875	529	240	3243	1529
As	948	145	99.8	111	1.31–1.87	1–286	2.2	280,000	288	132	4.13	4.96	45.8	14.4
Ba	135	28.0	22.4	23.2	14.9–24.9	10–162			236	3043	23.2	33.9	84.0	32.7
Be	1.76	0.032	0.020	0.023	< 0.005	< 1			0.895	0.828	< 0.005	< 0.005	0.185	0.014
Bi	0.076	0.002	0.004	0.003	0.004–0.006	< 3	0.1	0.1	0.118	0.108	0.004	0.018	0.042	0.033
Cd	0.364	0.017	0.030	0.008	0.004–0.007	0.02–0.1	< 2	3650	0.269	0.636	0.030	0.021	1.34	1.22
Co	8.95	0.088	0.044	0.054	0.06–0.08	< 0.1	0.4	8700	9.21	20.6	0.203	0.160	3.73	2.69
Cr	14.9	0.956	0.707	0.768	0.38–0.52	< 5	0.9	3230	178	86.7	1.76	0.801	18.4	2.04
Cs	7.80	1.23	0.931	1.01	< 0.002	0.1–106			7.12	3.32	0.118	0.103	1.55	0.830
Cu	12.4	0.951	0.768	0.618	0.38–0.51	0.4–10	3.2	12,200	23.7	10.1	0.811	0.769	24.6	21.8
Fe	6567	67.3	31.7	52.5	4.0–11	40–140	100	7,886,000	12,011	16,289	314	140	3464	591
Li	5.70	2.22	1.57	1.65	1.00–1.30	1–270			5.00	5.71	0.185	0.377	2.33	1.14
Mn	571	4.77	2.49	3.06	6.70–15.9	0.5–90	20	315,030	583	719	21.6	30.2	240	155
Mo	0.920	0.879	0.502	0.566	0.82–1.70	0.2–3.5	0.2	35	1.15	0.807	0.18	0.04	0.565	0.358
Ni	53.4	1.47	1.03	1.00	0.58–0.95	0.9–5.7	10	8190	95.6	66	1.76	1.00	12.9	9.34
Pb	10.3	0.178	0.158	0.106	0.042–0.057	0.005–2	< 30	2070	12.6	12.4	0.360	0.578	4.91	1.84
Rb	13.4	5.13	3.88	4.23	0.69–0.94	0.8–63			28.5	25.6	0.730	0.603	12.2	8.59
Sb	51.4	13.5	10.7	11.3	0.04–0.05	0.09–10.6	0.4	10.8	73.2	84.1	2.47	0.902	17.5	2.06
Se	0.607	0.535	0.186	0.107	0.05–0.13	0.2–2			0.86	0.05	< 0.05	< 0.05	0.347	0.330
Sn	0.128	0.071	0.062	0.081		< 1			0.62	0.532	0.244	0.331	0.560	0.406
Sr	246	167	127	136	0.05–0.11	62–917			135	228	203	270	83.3	29.9
Ti	79.5	1.05	0.387	0.851	< 0.30	2.5–9.4			777	845	16.4	12.7	218	49.7
Tl	21.8	0.668	0.581	0.568	0.003–0.005	0.10–0.40	0.2	0.2	11.3	14.1	0.443	0.386	4.38	2.48
U	1.54	0.444	0.311	0.371	1.70–3.70	0.21–0.70	0.5	541	1.98	2.05	0.047	0.050	0.750	0.415
V	11.4	0.760	0.536	0.578	0.88–1.30	0.1–2			34.6	25.8	0.693	0.402	7.21	1.17
Zn	40.9	9.68	1.98	5.53	0.67–1.20	0.5–23.5	20	9830	58.6	129	11.7	25.4	100	102

[a] GR - range of values reported by FOREGS for nearby area (Salminen et al., 2005).

[b] ThW – values for thermal waters from Kožuf mountain (Boev and Jančev, 2014).

[c] A2 - Majdanska River – upstream from mineralisation, A4 – standing water in adit in Allshar (Alderton et al., 2005).

concentrations conditioned by local mineralization. Measured concentrations for a number of elements (Ba, Be, Bi, Cd, Co, Cr, Cu, Li, Mn, Mo, Ni, U and V) were found in accordance with available FOREGS data (Salminen et al., 2005). On the other hand, As, Cs, Fe, Pb, Rb, Sb, Sr, Ti, Tl and Zn were found at much higher levels compared to other streams in the region. While for Fe, Pb, Rb, Sr, Ti, and Zn obtained concentrations for the Majdanska River water were few times higher compared to the available FOREGS data, levels of As, Cs, Sb and Tl were one to two orders of magnitude higher than for other streams in the region. For Ag, Se and Sn FOREGS data are not available for the stream water and could

not be discussed.

Water sample 1, at the site of discharge of acid mine drainage in the Majdanska River, exhibits significantly higher element concentrations compared to all other water samples. Only for molybdenum, comparable values were obtained. For all other elements, concentrations were 2 to 180 times higher in sample 1 than in other water samples. For As, Ba, Cs, Li, Rb, Sb, Se, Sn, Sr, U and Zn, concentrations were two to eight times higher; for Ag, Be, Bi, Cd, Cr, Cu, Ni, Pb, Tl and V concentrations were up to two orders of magnitude higher, while Al, Co, Fe, Mn, and Ti displayed hundred to two hundred times higher concentrations in
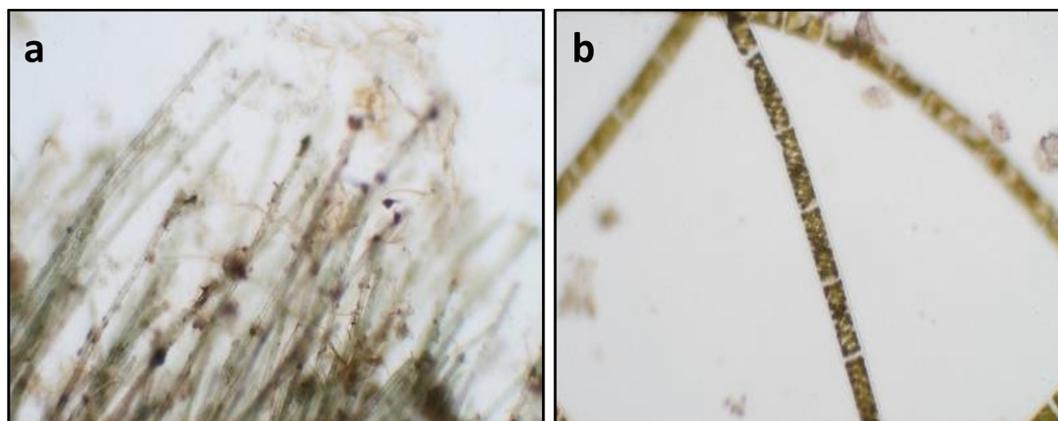

Fig. 4. The examined biota community is composed of algae *Audouinella* sp. (a) and *Spirogyra* sp. (b).
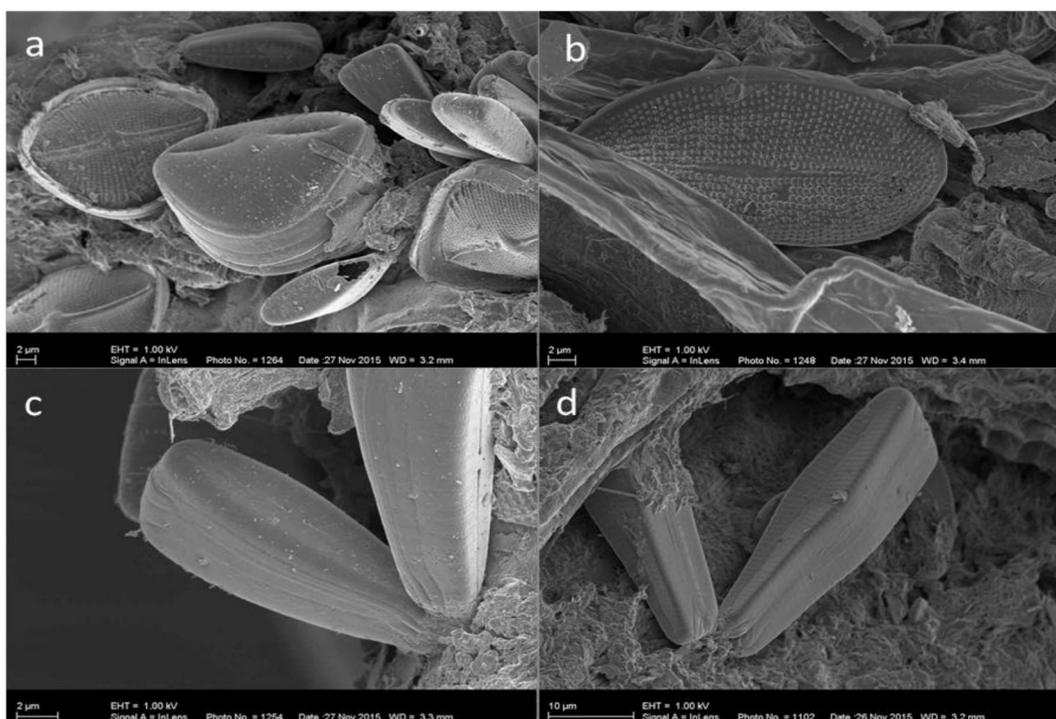
Fig. 5. Dominant diatom species in periphyton developed on algae: a) *Cocconeis pediculus* Ehr., b) *Cocconeis placentula* Ehr., c) *Gomphonema minutum* (C.A.) C. Agardh, and d) *Gomphonema subclavatum* (Grun.) Grun.

Table 2
Species occurrence frequency (F), Trophic Diatom Index (TDI) and Saprobic Index (SI) from periphyton communities.

Taxa	F (%)	TDI	SI
Cocconeis pediculus Ehrenberg	76	2.5	1.8
Cocconeis placentula Ehrenberg	82	2.5	1.8
Cocconeis pseudolineata (Geitler) Lange-Bertalot	27	2.3	2.0
Gomphonema minutum (C. Agardh) C. Agardh	56	2.8	2.2
Gomphonema subclavatum (Grunow) Grunow	62	2.0	2.2
Navicula tripunctata (O.F. Müller) Bory	24	2.6	2.0
Navicula veneta Kützing	18	3.0	2.8
Nitzschia fonticola (Grunow) Grunow	16	3.0	2.0
Nitzschia sp.	8	3.2	2.3
Planothidium lanceolatum (Bréb. ex Kütz.) Lange-Bertalot	22	2.0	1.8
Rhoicosphenia abbreviata (C. Agardh) Lange-Bertalot	9	2.7	2.1
Ulnaria biceps (Kützing) Compère	11	3.0	1.9

sample 1 compared to other water samples (Table 1).

Nonetheless, wide range of concentrations in studied water samples were found to be in accordance with element levels reported for "thermal mineral water" from the Kožuf Mountain, fed largely by the Majdanska River (Table 1; Boev and Jančev, 2014). Increased content of certain elements, especially As, Ba, Cs, Rb, Sr, and U, in the thermal mineral water from Kožuf Mountain was attributed to the increased amount of these elements in the surrounding rocks (Boev, 1988; Boev and Jančev, 2014).

Algae samples also displayed some differences in trace element distribution. For Al, Be, Bi, Fe, Li, Mn, Mo, Ni, Pb, Rb, Sb, Sn, Ti, Tl, U and V both algae species displayed comparable concentrations (Table 1). However, levels of Ag, As, Cr, Cs, Cu and Se were found higher in *Audouinella* sp. (by a factor of 1.5–2.4) than in *Spirogyra* sp. On the other hand, in *Spirogyra* sp. values of Ba, Cd, Co, Sr and Zn were higher (by a factor of 1.4–12.9) than in *Audouinella* sp. An overall highest difference between these two algae was observed for Ba which was found at almost thirteen times higher concentrations in *Spirogyra* sp. than in *Audouinella* sp.

The obtained values for Cr, Ni and Pb in *Spirogyra* sp. were found to be in accordance with literature values for *Spirogyra* sp. from the Shoor River (Iran) (Hamidian et al., 2013), an area influenced by local agri-culture and Mn mining activities. Interestingly, levels of Al, Cd, V and Zn in the Majdanska River samples were several times lower compared to Shoor River samples, while As, Cu, Fe and Mn displayed much higher values, two to seven times higher than in *Spirogyra* sp. from the Shoor River. Previous studies reported on high accumulation abilities of the algae *Spirogyra* sp. for different metals, e.g. Cr (Gupta et al., 2001; Hamidian et al., 2013), Cu, Mn, Pb and Zn (Rajfur et al., 2011), Fe and Zn (Hamidian et al., 2013), and Mg, V, As, and Cd and Cr (Hamidian et al., 2013). However, metal biosorption by *Spirogyra* sp. was found to be dependable, not only on various environmental factors, but also on the algal taxon, age of alga, and seasonal variation (Haritonidis and Malea, 1999; Novis and Harding, 2007; Das et al., 2008).

Snail samples (both shell and tissue) displayed some differences in the levels of certain elements. In general, trace elements reached greater concentrations in soft tissues than in shells; with exception of Sr which is readily incorporated along with Ca and Mg into the snail shells. Average element levels were 2 to 50 times higher in the soft tissues, with the overall highest average enrichments observed for Cs (11×), U (12×), Rb (16×), Co (18×), Cu (29×) and Cd (50×). Significant variation in element concentrations between shell and tissue, where tissue concentrations were much higher than the ones in the shell, was found to be in accordance with previous findings on gastropods (e.g. Cravo et al., 2004).

Algae are often used as biological sensors for detecting potential toxic effects of various inorganic and organic pollutants, including heavy metals (Brayner et al., 2011; Durrieu et al., 2011). Their ability to take up and accumulate heavy metals from their surrounding en-vironment (De Philippis et al., 2011; Mishra et al., 2011; Vogel et al., 2010; Kumar and Oommen, 2012) is well documented. Gastropods are also known to easily accumulate pollutants, such as heavy metals (Beeby and Eaves, 1983; Lau et al., 1996; Jordaens et al., 2006), and due to their feeding behaviour they are considered to be exposed to increased contamination and consequently accumulate higher levels of heavy metals compared to their environment. Conditions of metal
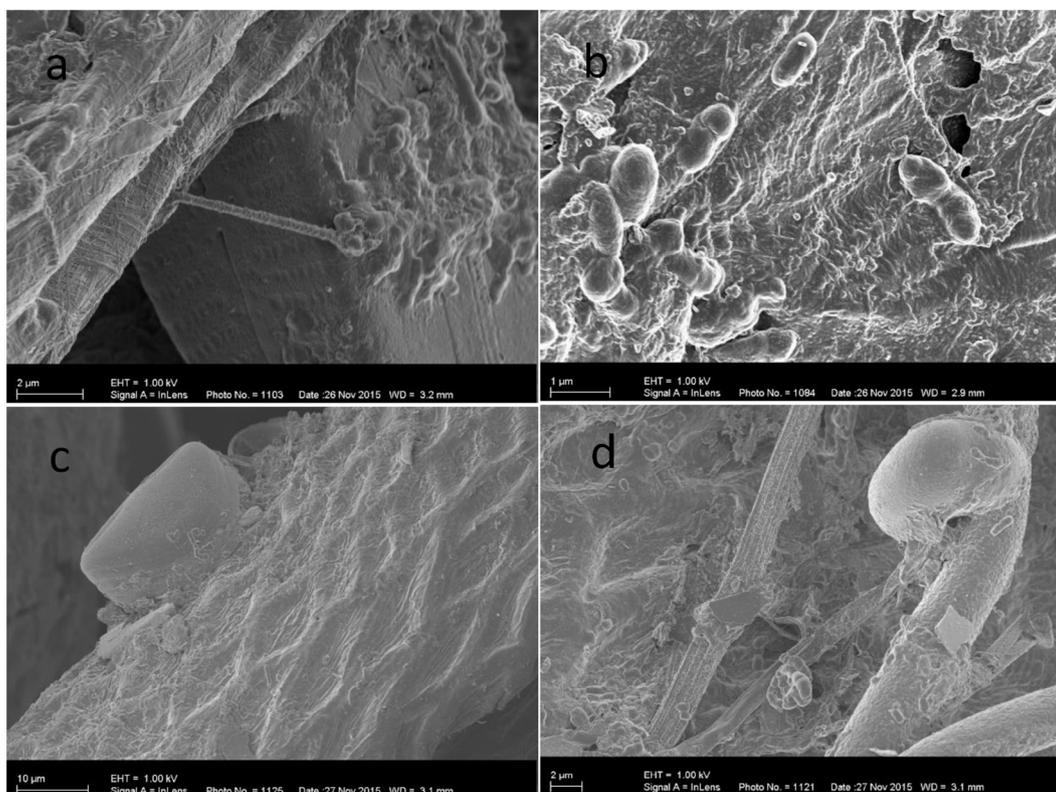
Fig. 6. Micro-colonies of bacteria formed on the surface of diatom (a) and algae (b, c, d).

accumulation in both algae and snails are discussed in more detail in Sections 3.5.2 and 3.6.

3.4. Bacteriological analysis

The abundance of bacteria in water, sediment and freshwater snail *Radix labiata* from Majdanska River is shown in Table 3. The numbers of total heterotrophic bacteria were in usual range for environmental samples (Ehrlich and Newman, 2009). Carbapenem-resistant bacteria were found in water, sediment and snails living in this metal-contaminated environment. The bacterial resistance to carbapenems is linked to their resistance to heavy metals, as shown for Zn and Cu in *Pseudomonas aeruginosa* (Caille et al., 2007). Therefore, the carbapenem resistance in this environment without the anthropogenic influence is most probably intrinsic. The latter is known to be present in the environmental bacterial species such as *Stenotrophomonas* spp. The number of total heterotrophic bacteria and carbapenem-resistant bacteria is significantly higher in the river sediment as compared to the river water, and particularly in *Radix labiata*, suggesting the accumulation of bacteria in sediment and snail tissue.

Table 3
Numbers of total heterotrophic bacteria and carbapenem-resistant bacteria (CRB) in samples of water, sediment and freshwater snail *Radix labiata*, presented as mean values and standard deviations per 1 mL of water or 1 g of sediment and *R. labiata*.

Sample	Heterotrophic bacteria (log CFU/mL or g)	CRB (log CFU/mL or g)
Water	4.8 ± 0.2	−0.5 ± 0.2
Sediment	7.2 ± 0.2	2.1 ± 0.0
R. labiata	8.6 ± 0.2	4.8 ± 0.0

3.5. Discharge of acid mine drainage into the Majdanska River

The highly acidic water (pH = 2.3) in a passageway of the Allchar mine (Alderton et al., 2005) appears to be the cause for the nature of underground mine water in the discharge area. Underground mine waters, i.e. AMD, with pH values lower than those of the river water, are discharged into the Majdanska River (Table 1). This geochemical barrier causes significant changes in the mobility of ionic species, due to changes in speciation and redox shift and new hydrolysis products. The term "Dilution-Retention factor" is applied as a simple expression for the decrease of contaminant load after mixing of discharge spring water and the Majdanska River. Dilution-Retention (Retardation) factor D asserts semi-quantitatively both effects dilution and chemical retention (D = X1 / X2; X1 = concentration of an element in the discharge spring water at site 1, and X2 = concentration in Majdanska River after dilution at site 3, Table 4). The D factors are discussed in more detail for each individual element in the Section 3.5.1.

3.5.1. Abiotic response to increased levels of toxicants

To evaluate the variation and general decrease of toxicant concentrations after the mixing of acidic mine water with river water, standard physico-chemical equilibration criteria have been applied for 25 °C and 1 bar pressure. Considering the elevated concentrations of As and Tl in the investigated area, which is also reflected in the geochemistry of the examined water samples, special attention has been paid to these elements in the following discussion.

The lowest D values (from 1.94 to 8.38) were obtained for Sr, Li, Rb and Cs (Table 4). This is somewhat expected, given the conservative nature of these elements in aqueous medium.

Low D values (from 2.06 to 9.50) were also calculated for oxyanion-forming elements As, Sb, Se, Sn and U. Their negative charge stays in repulsive relation with deprotonised surfaces of colloids, inhibiting adsorption. Thus, their high mobility in existing oxidising conditions at Eh = 0.17 V is reflected in small D values, ruling out the significant

Table 4

Calculated Dilution-Retention factors (D) for water and Bioconcentration (BCFs) and Bioaccumulation (BAFs) factors for algae and *Radix labiata*.

Element	D factor	BCFs		BAFs	
		Audouinella sp.	*Spirogyra* sp.	Shell	Tissue
Mo	1.83	1.8	1.3	0.2	0.7
Sr	1.94	0.9	1.6	1.7	0.4
Sn	2.06	8.5	7.3	3.9	6.6
Se	3.26	3.6	0.2	–	1.4
Rb	3.45	6.5	5.9	0.2	2.4
Li	3.63	2.8	3.1	0.2	1
Sb	4.8	6.2	7.2	0.1	0.8
U	4.95	5.3	5.5	0.1	1.6
Ba	6.03	9.7	125	1.2	2.4
Cs	8.38	6.8	3.2	0.1	1.1
As	9.5	2.4	1.1	0.04	0.3
Cd	12.1	16.3	38.5	1.5	77.4
Cu	16.1	30.6	13.1	1	30
Bi	19	36.3	33.2	3.4	11.5
Zn	20.7	12.1	26.6	3.8	20.9
Cr	21.1	224	109	1.6	12.9
V	21.3	56.5	42.1	0.9	6.8
Tl	37.5	18.8	23.5	0.7	5.7
Ag	43.6	3.6	2	2.2	6.9
Ni	51.8	76.5	52.8	1.1	8.9
Pb	65.2	95.8	94.3	3.6	25.7
Be	88	37.3	34.5	–	4.2
Al	157	28.8	27.9	12.3	76.2
Co	203	162	361	3.2	56.3
Ti	205	1189	1294	22.2	205
Fe	207	259	351	4.9	43.7
Mn	229	183	226	8.1	62

The BCF and BAF values have to be multiplied by 10^3 to attain bioconcentration and bioaccumulation since element concentration in the water is expressed in $\mu g\,L^{-1}$ and in algae and snail is expressed in $\mu g\,g^{-1}$.

effect of adsorption retention, only invoking dilution.

The D values for As, Sb, Se, Sn, and U, in increasing order are:

Sn (2.06) < Se (3.26) < Sb (4.80) < U (4.95) < As (9.50)

As stated previously, $H_3AsO_4^0$ and $H_2AsO_4^-$ are dominant forms under acidic conditions in AMD from Allchar ore deposit.

The reaction of As(V) oxidation:

$H_3AsO_3 + H_2O = H_2AsO_4^- + 3H^+ + 2e^-$

Based on the Nernst equation and using data for Eh and pH from Table 1, the ratio As(V)/As(III) was calculated. Successive steps used in the calculations are explained in Appendix A.

$\Delta G°_r = 123.52\,kJ$ (29.51 kcal) ($\Delta G°_f$ taken from Robie et al., 1978, and Wagman et al., 1982)
$E° = +0.64\,V$
0.183 (V) = 0.64 (V) − 0.0885 pH + 0.0295 log $aH_2AsO_4^-$ − 0.0295 log aH_3AsO_3
log $H_2AsO_4^-/H_3AsO_3 = 7.36$; $H_2AsO_4^- / H_3AsO_3 = 2.3 \times 10^7$

The ratio of As(V)/As(III) = 2.3×10^7 in the discharge spring water is highly in favour of oxidised form, although "equilibrium" conditions should be taken with caution. Arsenic acids and their ionization products are the primary carrier of As and their negative charges are not compatible with negative charges on the deprotonized colloids, evident in the low value of D = 9.50. The PO_4^{3-} and SO_4^{2-} ions compete efficiently with AsO_4^{3-} for adsorption sites and also interfere in cell metabolism of algae and affect value of As(V)/As(III) ratio (more in Section 3.5.2).

On the other hand, elements prevalently present as divalent cations in water, Be, Ba, Cd, Co, Cu, Ni, Pb and Zn displayed higher D values, ranging from 6.03 to 203.

The D values for Ba, Be, Cd, Co, Cu, Ni, Pb, and Zn, in increasing

order are:

$Ba^{2+}(6.03) < Cd^{2+}(12.1) < Cu^{2+}(16.2) < Zn^{2+}(20.7) < Ni^{2+}(51.8)$
$< Pb^{2+}(65.2) < Be^{2+}(88.0) < Co^{2+}(203)$
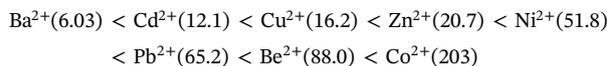
The only exception in the sequence of increasing D factors of divalent metals is Ba^{2+} with small D values (6.03). The behaviour of barium is controlled by several reaction pathways, such as bioconcentration and biomineralisation processes (see Section 3.6 on biomineralisation). The only slight decrease in Ba concentration can be linked to abiotic effects like complexation of magnesium as $MgSO_4^0$. Namely, acidic spring water encounters high $MgSO_4^0$ as a result of dolomite dissolution at the site of ore weathering (Strmić Palinkaš et al., 2018). The formation of $MgSO_4^0$ complex increases barite solubility by a factor of 5 over a range of magnesium concentration from 0 to 0.1 mol/L (2430 mg/L) (Deutsch, 1997). Constant conductance values between 163.3 μS/cm and 169.8 μS/cm indicate that a decrease of ionic strength is not expected (Table 1). Besides, the surface complexation constant for Ba^{2+} on ferric oxide (log $KBa^{2+} = -7.2$) is low (Deutsch, 1997; Dzombak and Morel, 1990).

Similar to divalent cations, the D values calculated for Bi, Cr, V and Tl ranged from 19.0 to 37.5 and presented in increasing order are:

Bi (19.0) < Cr (21.0) < V (21.3) < Tl (37.5)

The high positive charge of bismuth oxo-complexes ($Bi_6O_6^{6+}$) predominating at low pH enables efficient coprecipitation with iron oxyhydroxide. Relatively high D value (D = 19.0) for bismuth suggests its efficient removal from the water column, presumably by co-precipitation with mentioned iron hydroxides. The same is expected for Cr hydrolysis products, $Cr(OH)^{2+}$, $Cr(OH)^+$ and $Cr(OH)_3$, behaving as other trivalent cations and co-precipitating readily with iron hydroxide. Vanadyl ion (VO^{2+}), dominant form at lower pH, is also adsorbed on ferric hydroxide, at the discharge spring due to pH barrier, as evidenced by high D value (D = 21.3).

According to Tremel et al. (1997) monovalent thallous cation occurs almost exclusively in natural waters. The solubility of thallous compounds is high as monovalent thallium is readily transported through aqueous routes into the environment. Lin and Nriagu (1999) reported, however, a contradicting observation that 66–68% of the total dissolved thallium in the Lake Michigan and in two rivers Raisin and Huronof are in trivalent form. This equilibrium is applicable to the dilute waters with low concentration of ligands. Mine waste waters, however, are loaded with SO_4^{2-} with concentration which exceeds the thallium one after oxidation of sulphides. The Tl(III) engagement goes via $TlSO_4^+$ complex ion, stable under low pH and Eh, and shifts total dissolved thallium to thallic domain (log $KTlSO_4^+ = 9.2$). Thermodynamically, the Tl^{3+} would be used up and replaced at the expense of Tl^+ (Cheam, 2000). Adsorption of Tl^{3+} by iron hydroxide or eventually formation of thallic colloids would have the same affect.

$Tl^+ = Tl^{3+} + 2e^-$
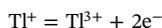
Based on the Nernst equation and using data for Eh and pH from Table 1, the ratio Tl(III)/Tl(I) was calculated.

$E° = +1.28\,V;$
$0.183(V) = 1.28(V) + 0.0295$ log Tl^{3+}/Tl^+

The acidity and redox parameters of the studied discharge spring water are pH = 7.76 and Eh = 0.183 V, and thus define the ratio of $Tl^{3+}/Tl^+ = 10^{-37.2}$ and, along with high D value, corroborate the prevalence of Tl^+ in studied water and its adsorption on colloid particles.

Similar observations were reported for streams near the Pb–Zn Carnoulès mine (southern France) (Casiot et al., 2011). Thallium concentration reached 534 μg L^{-1} in the Reigous acid mine drainage downstream from the abandoned Pb–Zn Carnoulès mine. It decreased to 5.44 μg L^{-1} in the Amous River into which the Reigous creek flows,

with Tl(I) predominating (> 98% of total dissolved Tl), mainly in the form of Tl^+ and $TlCl_2^+$ (Casiot et al., 2011).

High concentrations of Al ($3169 \mu g \, L^{-1}$, 1.34×10^{-4} mol/L), Ti ($79.5 \mu g \, L^{-1}$, 1.66×10^{-6} mol/L), Fe ($6567 \mu g \, L^{-1}$, 1.18×10^{-4} mol/L) and Mn ($571 \mu g \, L^{-1}$, 1.04×10^{-5} mol/L) in spring water, and a substantial increase of D factors (from 157 to 229) for these elements, a simple measure of the immobility, implies their precipitation.

The D values for Al, Fe, Mn, and Ti in increasing order are:

Al (157) < Ti (205) < Fe (207) < Mn (229)

The next step was to impose saturation and super-saturation criteria to identify the colloid precipitate which controls trace metal co-precipitation/adsorption of divalent cations (Gaillardet et al., 2003). A step forward is to calculate Saturation index of hydroxides SI = log(a_1 / a_{sat}), whereas a_1 is measured activity of trivalent cation at the site 1 (pH 7.62, Eh 0.183 V), and its equilibrium activity a_{sat} by the same parameters (Appendix A). Thermodynamic reasoning in given the Appendix A using data from Latimer (1952), Bricker (1964), Wagman et al. (1968, 1969), Tremaine and LeBlanc (1980) and Garvin et al. (1987).

Super-saturation prefers higher precipitation rate for titanium (SI $TiO(OH)_2$ = 10.8) and iron (SI $Fe(OH)_3$ = 3.4), compared to aluminium hydroxides with slight saturation conditions (SI $Al(OH)_3$ = 0.24). Only manganese hydroxides displayed under-saturated conditions (SI MnO(OH) = −4.3). Realistic order of precipitation under turbulent hydrodynamic conditions by mixing discharge water and river water, however, is not conceivable. The Fe and Ti hydroxide colloids, which attain significant saturation, have different adsorption capacity and rate-controlling sol-flocculation formation, which depends primarily on different zero charge point, and transfers from positive to negative electric charge on the colloid surface (Gaillardet et al., 2003).

The Al and Mn owe their high D factors to co-precipitation with sols or flocculated colloids of iron rather than titanium. Co-precipitation reaction can be defined as:

$$Fe^{2+} + Mn^{2+} + 6H_2O = 2(Fe, Mn)(OH)_3 + 6H^+ + 2e^-$$
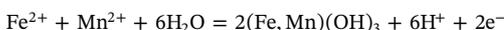
Dissolved cations in acidic waters are thus considered to be rapidly scavenged through adsorption by iron hydroxide. The iron colloids are preferred to titanium ones, as a major sink for divalent cations, due to dominant iron concentration and colloid volume capacity. Obviously, it does not proceed in the base flow of the saturated zone due to low pH conditions (Fig. 7).

3.5.2. Impact on biota

To clarify the conditions of metal accumulation in algae and snails inhabiting the Majdanska River, bioconcentration factors (BCFs) and bioaccumulation factors (BAFs) were calculated as the ratio of toxicant concentrations in the biological sample (algae, snail shell or snail tissue) to its average concentration in the water, BCF = C_{algae} / C_{water} and BAF = C_{snail} / C_{water} (Table 4). The BCF and BAF factors values have to be multiplied by 10^3 given that element concentration in the water is expressed in $\mu g \, L^{-1}$, and in algae and snails in $\mu g \, g^{-1}$. To clarify these two terms, *bioaccumulation* occurs within an organism, where a certain substance builds up in the tissue and is absorbed faster than it is removed from it. Bioaccumulation often occurs in two ways, simultaneously: by eating contaminated food, and by absorption directly from water. This second case is specifically referred to as *bioconcentration* (Arnot and Gobas, 2004).

According to calculated BCFs (Table 4), bioconcentration of As, Cr, Cs, Cu, and Se was preferred in *Audouinella* sp., while Ba, Cd, Co, Sr, and Zn accumulated more in *Spirogyra* sp.

A similar set of elements (Al, Bi, Cd, Co, Cr, Cu, Fe, Mn, Pb, Ti and Zn) displayed elevated BAF factors in the snail tissue, with an overall highest value calculated for Cd (77.4), Al (76.2) and Ti (205). Nonetheless, BAF factors for snail tissue were higher than those BCFs observed for algae only for Al, Ag, Cd, Se and Zn (Table 4). For all other
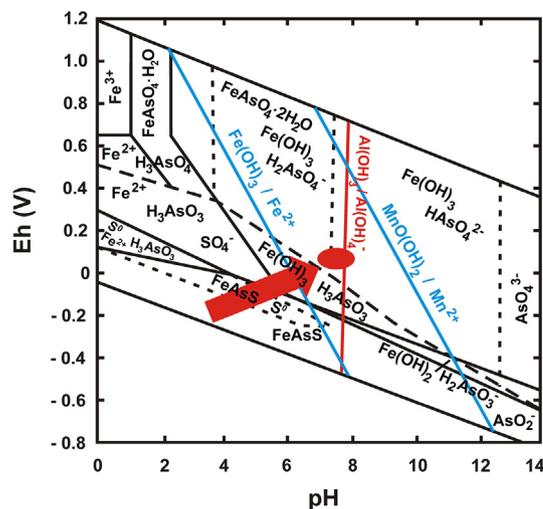

Fig. 7. Eh-pH diagram for the As-Fe-S-H_2O system depicts rapid change in Eh-pH conditions after discharge of spring acid water into Majdanska River at 25 °C and 1 bar pressure (diagram modified and accomplished after, Bhakta et al., 1989). Calculated boundaries for As activities [10^{-5} mol/L]; blue lines for Fe^{2+}/$Fe(OH)_3$ [10^{-4} mol/L] and Mn^{2+}/$MnO(OH)_2$ [10^{-5} mol/L]; and red line for saturation concentration of $Al(OH)_4^-$/$Al(OH)_3$ [10^{-6} mol/L] at pH 7.76. Red dot represents chemical conditions at the discharge site 1. (For interpretation of the references to colour in this figure legend, the reader is referred to the web version of this article.)

elements, BCF factors were higher in algae than BAFs for snails.

The latter suggests that both algae species have great ability to accumulate elements from the environment (Table 4). Since the algae are primary producers they take up metals from enriched sediment and water by bioconcentration. Bioaccumulation of metals should be expected in snails grazing algae. However, the analysed snails, collected from the same place and presumably fed by algae, showed no significant accumulation of elements compared to *Spirogyra* sp. and *Audouinella* sp. indicating that the snail's diet is not exclusively algae. During the dry period, more grass or other plant material is available. Toxic metal levels in different snail organs would likely provide a better understanding of bioaccumulation mechanisms. Active self-remediation by excretion of toxicants is a possible alternative.

3.6. Biomineralisation, bioconcentration, and bioaccumulation

The foregoing descriptive presentation offers some additional observations using the diagram in Fig. 8 (logarithms of BCFs, BAFs and D factors). The diagram shows several features that are likely related to the hydrogeochemical conditions in the Majdanska River.

While the carbonate bedrock controls the pH in the river water by effective buffering, it seems that biomineralisation and bioconcentration of algae exerts control on toxicants along the entire river flow. Epicellular biomineralisation of oxyhydroxides on algae scavenges toxicants and contributes to their depletion. An increase in pH by buffering effect of carbonate rocks is supported by dissimilatory usage of CO_2 and rise of Eh by oxygen, both result of algal photosynthesis. The snails take active part by consuming dead algal matter, a possible cause of oxygen deficiency due to bacterial decomposition. As generally known and confirmed by bacteriological analysis, the ecosystem of the Majdanska River is teeming with bacteria.

3.6.1. Epicelullar biomineralisation of oxyhydroxides

The D factor steadily grows (Fig. 8) from monovalent cations to elements that form oxyhydroxides governed by thermodynamic principles of abiotic control of solute mobility. It expresses retarded mobility of different species soon after mixing of acid discharge and river
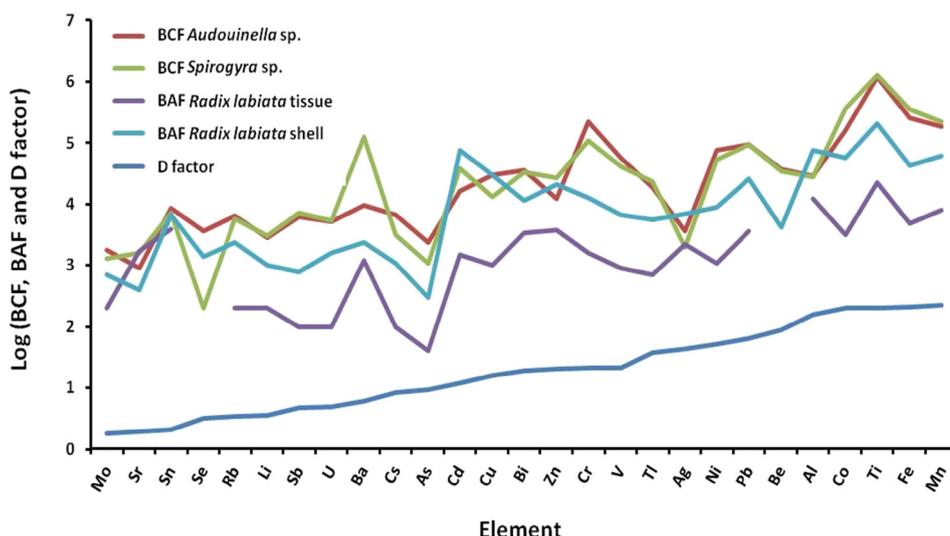
Fig. 8. BCF, BAF, and D factors for measured elements in observed organisms and water.

water. The BCFs $\times 10^3$ of algae for Fe (259, 351), Mn (183, 226) and Ti (1189, 1294) have the highest values, implying oxyhydroxides biomineralisation as a product of extracellular deposition on the cell walls of organic matrices. The epicellular biofilms grow by heterogeneous nucleation of hydroxide on the deprotonated surface, under near-neutral pH. Preconcentration of Fe(II) on carboxyl and phosphate groups have a catalytic effect (Bayramoğlu et al., 2006), increasing rapidly the rate of deposition from saturated solution. The algae favour kinetic over thermodynamic reaction control, precipitating oxyhydroxides and co-precipitating trace elements at the mixing site "discharge spring-river water". Nevertheless, along the river flow thermodynamic equilibrium promotes homogenous distribution of toxicants, keeping their level close to permissible values.

3.6.2. Intracellular biomineralisation of barium

An overall highest difference between the two taxa of algae was observed for Ba which was found at almost thirteen times higher concentrations in *Spirogyra* sp. (BCF $\times 10^3$, 125) than in *Audouinella* sp. (BCF, 9.7). Although collected at the same habitat on the same boulder, these two algae species apparently have different abilities to accumulate elements by their metabolism (Table 1). Barite precipitation by living organisms (protozoa) was demonstrated in lacustrine freshwater environments (Brook et al., 1980; Finlay et al., 1983). The phosphoryl and carboxyl groups in the structural polymers of the cell wall outer membrane may be sorbent constituents which play an important role in the precipitation process. Deprotonation of these groups provides discrete complexation sites for barium in solution. The high content of the SO_4^{2-} captures Ba ions, thus giving rise to the growth of barite nucleus (González-Muñoz et al., 2003). Such an interpretation favours epicellular accumulation of barium and formation of barite crystals inclusions.

The intracellular biomineralisation/barite inclusions were evidenced by Wilcock et al. (1989). They studied the unicellular desmid green algae *Closterium moniliferum*, which precipitate $BaSO_4$ crystals in small vacuoles at the tips of the cells. By use of SXRF microscopy they visualized the intracellular dynamics of Ca, Sr, Ba, and S and unravelled the mechanisms involved in the unusual selectivity exhibited by *C. moniliferum*. In this "sulphate trap" model, high sulphate levels and the presence of soluble Ba in the vacuole leads to precipitation of $BaSO_4$ (Fig. 9). High accumulation of barium (3 mg/g of dry biomass, Table 1) in *Spirogyra* sp. through intracellular biomineralisation implies its potential use in the remediation of waters polluted by barium.
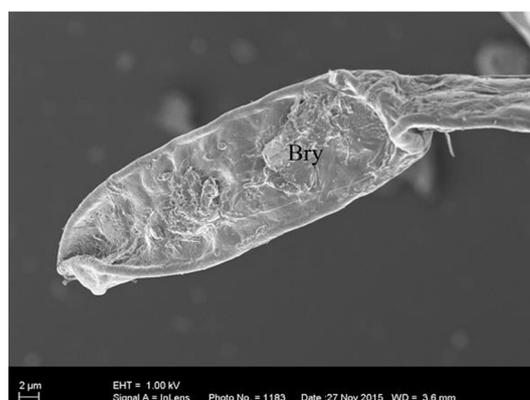
Fig. 9. SEM image of *Spirogyra* sp. High accumulation of Ba (3 mg/g of dry biomass) in *Spirogyra* sp. resulted in accumulation of intracellular inclusions of barite crystals (Bry).

3.6.3. Bioconcentration

Relatively high concentrations of Co, Cr and Ni in the investigated aquatic environment and biota are the result of the presence of ophiolites and nickel laterites within the hydrogeological ecosystem (Fig. 1b; Serafimovski et al., 2012), which causes the high BCFs in algae (Table 4). The applied analytical procedure does not allow differentiation of the bioconcentration by biosorption of the metals on biofilms or microbial mats from the bioconcentration by metabolic cell activity. The concentrations of other toxic metals, Bi, Cd, Pb, V and Zn, follow the same scheme of oxyhydroxides precipitation, which does not seem to be the case for arsenic and thallium. The decrease in their accumulation seems to be related to excretion from the cytoplasm by enzymatic activity.

Arsenic, one of the highly toxic contaminants in the Allchar arsenic mine attracts special attention. Surprisingly, its bioconcentration, in relative numbers (BCF $\times 10^3$, *Audouinella* sp., 2.4, and *Spirogyra* sp., 1.1), is one to two orders of magnitude lower than for other heavy metal toxicants like Zn (12.1, 26.6), Tl (18.8, 23.5), Cd (16.3, 38.5), Cu (30.6, 13.1), Bi (36.3, 33.2), V (56.5, 42.1), Ni (76.5, 52.8), Pb (95.8, 94.3), Co (162; 361), and Cr (224; 109). Algae readily methylate As(V) producing organic forms, dimethylarsinic acid (DMAA; $(CH_3)_2AsO(OH)$) and monomethylarsonic acid (MMAA; $CH_3AsO(OH)_2$) (e.g. Hasegawa et al., 2001). The As (III), and DMAA and MMAA are easily excreted from the cells keeping low concentration of As in algae (Hellwegerl et al., 2003). The amplitude of these processes depends on

115

the PO_4^{3-}/AsO_4^{3-} concentration ratio which directs the metabolism; methylation of pentavalent arsenic or reduction into As (III). Consequently, it changes seasonal As speciation and controls its bioconcentration.

Thallium is another harmful contaminant in the Allchar mine. It is also a highly toxic metal which does not seem to have any vital role in the metabolism of biota, including algae. Its bioconcentration is higher in relation to arsenic, but still lower than for some other metals. Obtained thallium levels were, however, comparable to those reported by Queirolo et al. (2009) for algae species *Myriophyllum acuaticum* ($0.295\,\mu g\,g^{-1}$ d.w. to $8.30\,\mu g\,g^{-1}$ d.w.) and Horned pondweed *Zannichellia palustris* L. ($0.615\,\mu g\,g^{-1}$ d.w. to $7.34\,\mu g\,g^{-1}$ d.w.) from La Cascada, Yalquincha, Ayquina and Rio Salado at Yerbas Buenas, Chile. High Tl values found in these species were related to local mining and smelter activities.

In general, logarithm of BCFs in the two taxa of algae, *Audouinella* sp. (18.8), and *Spirogyra* sp. (23.5) show a noticeable covariance (Fig. 8) for most elements, including thallium and arsenic. On the other hand, logarithm of BCFs in snail shell and tissue is not correlated with the element group in algae, although shell-tissue mutual correlation is well established.

4. Conclusion

The Majdanska River, flowing a fair part over carbonates, efficiently reduces the acidity of the water and controls toxicant concentrations at ecologically acceptable levels.

At the site of the spring inflow, Majdanska River mixes thoroughly with underground mine waters, raising Eh and pH close to the average river value. This geochemical barrier causes significant change in mobility of metal species, due to redox changes and new hydrolysis products. Saturation indices highlight the possibility of precipitation of Fe phases in the sediments of the river. Mixing of waters with contrasting chemical composition, therefore, involves complex interaction of dilution, adsorption and precipitation processes. Moreover, the output composition of water is additionally modified by biological processes.

While the carbonate rocks control pH in the river water by effective buffering, it seems that biomineralisation and bioconcentration of algae exerts control on toxicants along the entire river flow. The algae promote kinetic over thermodynamic reaction control, precipitating oxyhydroxides and coprecipitating trace elements at the mixing site "discharge stream-river water". Barium intracellular biomineralisation in algae, suspected by high BCF, is testified by SEM image. However, along the river flow thermodynamic equilibrium establishes homogenous distribution of toxicants, keeping their level close to permissible values. It gives a promising possibility for using *Spirogyra* sp. for phytoremediation of Ba in environmentally unacceptable conditions. Another use can be envisioned in exploration activity for ore prospection, as a biological pathfinder indicator for metal deposits associated with barite.

Acknowledgements

Appendix A. Calculation of Saturation index (SI) for Fe, Mn, Al, Ti hydroxides

The Nernst equation was used in order to obtain the element activity (a_{sat}) that is needed to compute the SI value with respect to $Fe(OH)_3$ and $MnO(OH)$ assuming that reactions (1) and (6), respectively, take place. Calculation of $\Delta G°_r$ of reactions (1) and (6) is needed to calculate Eh^0 and is computed using Eqs. (2) and (7).

In order to calculate saturation indices for Al and Ti hydroxides, assuming that reactions (10) and (12), respectively, take place, equilibrium constants were calculated according to Eqs. (11) and (13).

A.1. Precipitation of iron hydroxide, $Fe(OH)_3$, at pH 7.62 is controlled by reaction

$$3H_2O + Fe^{2+} = Fe(OH)_3 + 3H^+ + e^- \tag{1}$$

$$\Delta G°_r = \Delta G°Fe(OH)_3 - (\Delta G°Fe^{2+} + 3\Delta G°H_2O) = 106.32 \text{ kJ (25.4 kcal)} \tag{2}$$

Standard free energy of formation of $Fe(OH)_3$ accepted from Wagman et al. (1968, 1969), Fe^{2+} from Tremaine and LeBlanc (1980), and H_2O from Garvin et al. (1987).

Saturation was calculated by equations:

$$Eh = Eh° + RT/nF \times \ln(a^3H^+/aFe^{2+}) \tag{3}$$

$$Eh° = \Delta G°_r/nF; \tag{4}$$

(Eh is half-cell potential, Eh° standard half-cell potential, n is the number of electrons in the redox equation, R is the universal gas constant, T is 298.15 K (25 °C) and F is the Faraday constant).

$$0.183 \text{ (V)} = 1.1 \text{ (V)} - 0.177 \text{ pH} - 0.059 \text{ log } aFe^{2+} \tag{5}$$

$a_{sat}Fe^{2+} = 4.92 \times 10^{-8}$ mol/L is calculated activity of Fe^{2+} in equilibrium with ferric hydroxide at 0.183 V, and pH = 7.62.
Activity of Fe^{2+} at site 1 is a_1; $a_1 = 1.176 \times 10^{-4}$ mol/L; $a_1 / a_{sat} = 2.4 \times 10^3$.
Saturation index SI $Fe(OH)_3 = \log(a_1 / a_{sat}) = 3.4$, shows high super-saturation, which means that decrease in iron concentration from site 1 to site 3 is due to precipitation of iron hydroxide.

A.2. The same calculation has been performed for MnO(OH) (γ-manganite)

$$Mn^{2+} + 2H_2O = MnO(OH) + 3H^+ + e^- \tag{6}$$
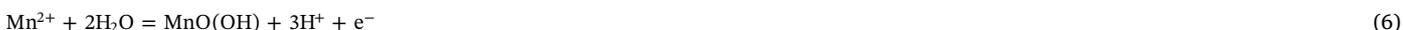
Standard free energy for Mn^{2+}; $\Delta G°Mn^{2+} = -227.7$ kJ $(-54.4$ kcal$)$ is from Latimer (1952), and MnO(OH), $\Delta G°MnO(OH) = -558.0$ kJ

(-133.3 kcal) from Bricker (1964).

$$\Delta G^{\circ}{}_r = \Delta G^{\circ} MnO(OH) - (\Delta G^{\circ} Mn^{2+} + 2\Delta G^{\circ} H_2O) = 143.6 \text{ kJ (34.3 kcal)} \tag{7}$$

Saturation was calculated by equation:

$$Eh = Eh^{\circ} + RT/nF \times \ln(a^3 H^+ / aMn^{2+}) \tag{8}$$

$$0.183 \text{ (V)} = 1.49 \text{ (V)} - 0.177 \text{ pH} - 0.059 \text{ log } aMn^{2+} \tag{9}$$

$a_{sat} Mn^{2+} = 0.20$ mol/L is calculated activity of Mn^{2+} in equilibrium with γ-manganite at 0.183 V, and pH = 7.62.

Activity of Mn^{2+} at site 1 is a_1; $a_1 = 1.04 \times 10^{-5}$ mol/L; $a_1/a_{sat} = 5.2 \times 10^{-5}$.

The saturation index SI MnO(OH) = $\log(a_1/a_{sat}) = -4.3$, shows that the discharge spring water is under-saturated. Under such circumstances, manganite is coprecipitated with iron hydroxide. Coprecipitation reaction could be perceived as:

$$Fe^{2+} + Mn^{2+} + 6H_2O = 2(Fe, Mn)(OH)_3 + 6H^+ + 2e^-$$
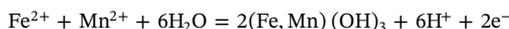
A.3. Above pH 7 dominating aluminium species in solution is Al(OH)$_4^-$ controlling saturation of Al(OH)$_3$
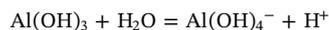
$$Al(OH)_3 + H_2O = Al(OH)_4^- + H^+$$
$$\Delta G^{\circ}{}_r = 67.0 \text{ kJ (16 kcal)}; \tag{10}$$

$$\log KAl(OH)_3 = -\Delta G^{\circ}{}_r (\text{kcal})/1.364 = -11.73 \tag{11}$$

$KAl(OH)_3 = aH^+ \times aAl(OH)_4^- = 1.86 \times 10^{-12}$; $a_{sat} Al(OH)_4^- = 7.76 \times 10^{-5}$ mol/L.

Activity of Al^{3+} at site 1 is a_1; $a_1 = 1.34 \times 10^{-4}$ mol/L; $a_1/a_{sat} = 1.73$.

SI Al(OH)$_3$ = $\log(a_1/a_{sat}) = 0.24$; it implies that discharge spring water at site 1 is slightly super-saturated, and aluminium might be precipitated as Al(OH)$_3$.

A.4. Precipitation of TiO(OH)$_2$ proceeds according to the following reaction

$$TiO^{2+} + 2 H_2O = TiO(OH)_2 + 2H^+ \tag{12}$$
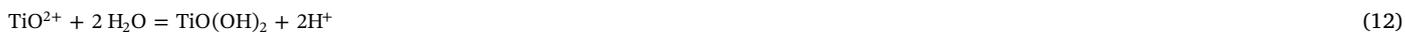
$\Delta G^{\circ}{}_r = -7.53$ kJ (-1.8 kcal);

($\Delta G^{\circ}{}_f$ stand. free energy of formation for TiO^{2+} and $TiO(OH)_2$ taken from Latimer, 1952).

$$\log KTiO(OH)_2 = -\Delta G^{\circ}{}_r (\text{kcal})/1.364 = 1.32 \tag{13}$$

$KTiO(OH)_2 = a^2 H^+ / aTiO^{2+} = 10^{1.32}$; $a_{sat} TiO^{2+} = 2.75 \times 10^{-17}$ mol/L;

Activity of Ti^{2+} at site 1 is a_1; $a_1 = 1.66 \times 10^{-6}$ mol/L; $a_1/a_{sat} = 6.04 \times 10^{10}$.

SI TiO(OH)$_2$ = $\log(a_1/a_{sat}) = 10.8$.

Saturation index SI confirms high super-saturation of TiO(OH)$_2$ and its possible precipitation.

References

Alderton, D.H.M., Serafimovski, T., Mullen, B., 2005. The chemistry of waters associated with metal mining in Macedonia. Mine Water Environ. 24, 139–149.

APHA, AWWA, WEF, 2005. Standard Methods for Examination of Water and Wastewater, 21th ed. American Public Health Association, New York.

Arnot, J.A., Gobas, F.A.P.C., 2004. A food web bioaccumulation model for organic chemicals in aquatic systems. Environ. Toxicol. Chem. 23 (10), 2343–2355.

Bačeva, K., Stafilov, T., Šajn, R., Tănăselia, C., Makreski, P., 2014. Distribution of chemical elements in soils and stream sediments in the area of abandoned Sb–As–Tl Allchar mine, Republic of Macedonia. Environ. Res. 133, 77–89.

Bačeva, K., Stafilov, T., Matevski, V., 2015. Distribution and mobility of toxic metals in *Thymus alsarensis* Ronniger in the Allchar As–Sb–Tl mine, Republic of Macedonia. Plant Biosyst. 149 (5), 884–893.

Baker, A.J.M., Reeves, R.D., Hajar, A.S.M., 1994. Heavy metal accumulation and tolerance in British populations of the metallophyte *Thlaspi caerulescens* J. & C. Presl (Brassicaceae). New Phytol. 127, 61–68.

Bayramoğlu, G., Tuzun, I., Celik, G., Yilmaz, M., Arica, M.Y., 2006. Biosorption of mercury(II), cadmium(II) and lead(II) ions from aqueous system by microalgae *Chlamydomonas reinhardtii* immobilized in alginate beads. Int. J. Miner. Process. 81 (1), 35–43.

Beeby, A., Eaves, S.C., 1983. Short-term changes in Ca, Pb, Zn and Cd concentrations of the garden snail *Helix asperaa* Muller from a central London car park. Environ. Pollut. A30, 233–244.

Bhakta, P., Langhans Jr., J.W., Lei, K.P.V., 1989. Alkaline Oxidative Leaching of Gold-bearing Arsenopyrite Ores. United States Department of the Interior (Report of investigations; 9258. Bibliography: pp. 12).

Boev, B., 1988. Petrological, Geochemical and Volcanic Features of Volcanic Rocks of the Kožuf Mountain (PhD Thesis). Faculty of Mining and Geology, Štip (in Macedonian).

Boev, B., Jančev, M., 2014. Geochemistry and origin of thermo-mineral waters of Kožuf Mountain Geol Macedonica. 28 (2), 165–174.

Boev, B., Serafimovski, T., 1996. General genetic model of the Allchar deposit Plate tectonic aspects of the Alpine Metallogeny in the Carpatho Balean Region. In: Proceedings of the Annual Meeting of IGCP Project 356. vol. 1. pp. 7585 (Sofia).

Boev, B., Bermanec, V., Serafimovski, T., Lepitkova, S., Mikulčić, S., Šoufek, M., Jovanovski, G., Stafilov, T., Najdoski, M., 2001–2002. Allchar mineral assemblage. Geol. Macedon. 15–16, 1–23.

Boev, I., Šorša, A., Boev, B., 2014. Trace Elements in the Onion Originated From the Tikves Area (Republic of Macedonia). Enigma, pp. 31–49.

Boev, B., Karakaseva, E., Boev, I., 2014. Geochemistry of the Endemic Flora Violla Allcharica and Thymus Allcharensis of the Allchar Site-Macedonia. Enigma, pp. 51–66.

Brayner, R., Couté, A., Livage, J., Perrette, C., Scard, C., 2011. Micro-algal biosensors. Anal. Bioanal. Chem. 401, 581–597.

Bricker OP (1964) PhD thesis, Dpt Geology, Harvard, University In: Garrels, RM and Christ, LC (1990).

Brook, A.J., Fotheringham, A., Bradly, J., Jenkins, A., 1980. Barium accumulation by desmids of the genus *Closterium* (Zygnemaphyceae). Br. Phycol. J. 15, 261–264.

Brookins, D.G., 1986. Geochemical behaviour of antimony, arsenic, cadmium and thallium, Eh-pH diagrams for 25 °C, 1 bar pressure. Chem. Geol. 54, 271–278.

Brookins, D.G., 1988. Eh-pH Diagrams for Geochemistry. Springer–Verlag.

Caille, O., Rossier, C., Perron, K., 2007. A copper-activated two-component system interacts with zinc and imipenem resistance in *Pseudomonas aeruginosa*. J. Bacteriol. 189 (13), 4561–4568.

Casiot, C., Egal, M., Bruneel, O., Verma, N., Parmentier, M., Elbaz-Poulichet, F., 2011. Predominance of aqueous Tl(I) species in the river system downstream from the abandoned Carnoulès Mine (southern France). Environ. Sci. Technol. 45 (6), 2056–2064.

Cheam, V., 2000. Comment on "Thallium Speciation in the Great Lakes". Environ. Sci. Technol. 34 (11), 2367–2368.

Chekroun, K.B., Baghour, M., 2013. The role of algae in phyto-remediation of heavy metals: a review. J. Mater. Environ. Sci. 4 (6), 873–880.

Chen, G., Dalton, C., Leira, M., Taylor, D., 2008. Diatom-based total phosphorus (TP) and pH transfer functions for the Irish Ecoregion. J. Paleolimnol. 40 (1), 143–163.

Cravo, A., Bebianno, M.J., Foster, P., 2004. Partitioning of trace metals between soft

tissues and shells of *Patella aspera*. Environ. Int. 30, 87–98.

Das, N., Wimala, R., Karthika, P., 2008. Biosorption of heavy metals: an overview. Indian J. Biotechnol. 7, 159–169.

De Philippis, R., Colica, G., Mecarozzi, P., 2011. Exopolysaccharide-producing cyanobacteria in heavy metal removal from water: molecular basis and practical applicability of the biosorption process. Appl. Microbiol. Biotechnol. 92, 697–708.

Deutsch, W.J., 1997. Groundwater geochemistry: fundamentals and applications to contamination. Lewis Publishers, Boca Raton, Fla.

Doi, H., Takagi, A., Kikuchi, E., 2007. Stream macroinvertebrate community affected by point-source metal pollution. Int. Rev. Hydrobiol. 92 (3), 258–266.

Durrieu, C., Guedri, H., Fremion, F., Volatier, L., 2011. Unicellular algae used as biosensors for chemical detection in Mediterranean lagoon and coastal waters. Res. Microbiol. 162, 908–914.

Dzombak, D.A., Morel, F.M.M., 1990. Surface Complexation Modeling: Hydrous Ferric Oxide. John Wiley & Sons, Science.

Ehrlich, L.H., Newman, D.K., 2009. Geomicrobiology, Fifth edition. CRC Press Taylor & Francis Group, New York, USA.

El Goresy, A., Pavičević, M.K., 1988. A new thallium mineral in the Allchar deposit in Yugoslavia. Naturwissenschaften 75, 37–39.

Ernst, H., Korschlnek, G., Kubik, P., Mayer, W., Morinaga, H., Nolte, E., Ratzinger, U., Henning, W., Kutschera, W., Muller, M., Schull, D., 1984. [205]Pb accelerator mass spectrometry of a very heavy radioisotope and the solar neutrino problem. Nucl. Inst. Methods Phys. Res. A B5, 426–429.

Escarré, J., Lefèbvre, C., Raboyeau, S., Dossantos, A., Gruber, W., Cleyet Marel, J.C., Frérot, H., Noret, N., Mahieu, S., Collin, C., van Oort, F., 2011. Heavy metal concentration survey in soils and plants of the Les Malines Mining District (southern France): implications for soil restoration. Water Air Soil Pollut. 216, 485–504.

European Commission, 2000. Directive 2000/60/EC of the European Parliament and of the Council of 23 October 2000 establishing a framework for community action in the field of water policy. Off. J. Eur. Communities 2000.

Evangelou, P.Y., 1998. Environmental Soil and Water Chemistry Principles and Applications. John Wiley & Sons, Inc. (564 pp.).

Fiket, Ž., Roje, V., Mikac, N., Kniewald, G., 2007. Determination of arsenic and other trace elements in bottled waters by high resolution inductively coupled plasma mass spectrometry. Croat. Chem. Acta 80, 91–100.

Fiket, Ž., Mikac, N., Kniewald, G., 2017. Mass fractions of forty-six major and trace elements, including rare earth elements, in sediment and soil reference materials used in environmental studies. Geostand. Geoanal. Res. 41 (1), 123–135.

Filipović Marijić, V., Raspor, B., 2012. Site-specific gastrointestinal metal variability in relation to the gut content and fish age of indigenous European chub from the Sava River. Water Air Soil Pollut. 223 (8), 4769–4783.

Finlay, B.J., Hetherington, N.B., Davison, W., 1983. Active biological participation in lacustrine barium chemistry. Geochim. Cosmochim. Acta 47, 1325–1329.

Freedman, M.S., Stevens, C.J., Horwitz, E.P., Fuchs, L.H., Lerner, J.L., Goodman, L.S., Childs, D.J., Hessler, J., 1976. Solar neutrinos: proposal for a new test. Science 193, 1117–1118.

Gaillardet, J., Viers, J., Dupré, B., 2003. Trace elements in river waters. In: Holland, H.D., Turekian, K.K. (Eds.), Treatise on Geochemistry. Elsevier, Amsterdam, pp. 225–272.

Garvin, D., Parker, V.B., White, H.J., 1987. CODATA Thermodynamic Tables Selectins for Some Compounds of Calcium and Related Mixtures: A Prototype Set of Tables. Hemisphere, New York.

González-Muñoz, T., Fernández-Luque, B., Martínez-Ruiz, F., Ben Chekroun, K., Arias, J.A., Rodríguez-Gallego, M., Martínez-Cañamero, M., de Linares, C., Paytan, A., 2003. Precipitation of barite by *Myxococcus xanthus*: possible implications for the biogeochemical cycle of barium. Appl. Environ. Microbiol. 69 (9), 5722–5725.

Goodyear, K.L., McNeill, S., 1999. Bioconcentration of heavy metals by aquatic macroinvertebrates of different feeding guilds: a review. Sci. Total Environ. 229, 1–19.

Gupta, V.K., Shrivastava, A.K., Neeraj, J., 2001. Biosorption of Cr(VI) from aqueous solutions by green algae *Spirogyra* species. Water Res. 35, 4079–4085.

Hamidian, A.H., Zareh, M., Poorbagher, H., Vaziri, L., Ashrafi, S., 2013. Heavy metal bioconcentration in sediment, common reed, algae, and blood worm from the Shoor river, Iran. Toxicol. Ind. Health 32 (3), 398–409.

Haritonidis, S., Malea, P., 1999. Bioaccumulation of metals by the green alga *Ulva rigida* from Thermaikos Gulf, Greece. Environ. Pollut. 104, 365–372.

Hasegawa, H., Sohrin, Y., Seki, K., Sato, M., Norisuye, K., Naito, K., Matsui, M., 2001. Biosynthesis and release of methylarsenic compounds during the growth of freshwater algae. Chemosphere 43, 265–272.

He, M., Wang, Z., Tang, H., 1997. Spatial and temporal patterns of acidity and heavy metals in predicting the potential for ecological impact on the Le An River polluted by acid mine drainage. Sci. Total Environ. 206, 67–77.

Hellwegerl, F.L., Farley, K.J., Dominic, M., Di Toro, D.M., 2003. Greedy algae reduce arsenate. Limnol. Oceanogr. 48 (6), 2275–2288.

Hendey, N.I., 1964. An Introductory Account of the Smaller Algae of British Coastal Waters. VI. Bacillariophyceae (Diatoms). Fishery Investigations. Her Majesty's Stationery Office, London (317 pp. + 45 plates).

Hering, D., Johnson, R.K., Krama, S., Schmutz, S., Szoszkiewicz, K., Verdonschot, P.F.M., 2006. Assessment of European streams with diatoms, macrophytes, macroinvertebrates and fish: a comparative metric-based analysis of organism response to stress. Freshw. Biol. 51, 1757–1785.

Hindák, F., Marvan, P., Komárek, J., Rosa, K., Popovský, J., Lhotský, O., 1978. Sladkovodné Riasy, 1st edition. Slovenské pedagogické nakladate'stvo, Bratislava.

Hrenović, J., Goić-Barišić, I., Kazazić, S., Kovačić, A., Ganjto, M., Tonkić, M., 2016. Carbapenem-resistant isolates of *Acinetobacter baumannii* in a municipal wastewater treatment plant, Croatia, 2014. Euro Surveill. 21 (15), 21–30.

Idaszkin, Y.L., Alvarez, M.D., Carol, E., 2017. Geochemical processes controlling the distribution and concentration of metals in soils from a Patagonian (Argentina) salt

marsh affected by mining residues. Sci. Total Environ. https://doi.org/10.1016/j.scitotenv.2017.04.065.

Ivanov, T., 1965. Zonal distribution of elements and minerals in the deposit Allchar. In: Symp. Problems of Postmagmatic Ore Deposition. II. pp. 186–191 (Prague).

Ivanov, T., 1986. Allchar the richest ore deposit of Tl in the world. In: Proceedings on the Feasibility of the Solar Neutrino Detection With [205]Pb by Geochemical and Accelerator Mass Spectroscopical Measurements, GSI-86-9, Darmstadt, (6 pp.).

Jakimska, A., Konieczka, P., Skóra, K., Namieśnik, J., 2011. Bioaccumulation of metals in tissues of marine animals, part I: the role and impact of heavy metals on organisms. Pol. J. Environ. Stud. 20 (5), 1117–1125.

Janković, S., Boev, B., Serafimovski, T., 1997. Magmatism and Tertiary Mineralization of the Kozuf Metalogenetic District, the Republic of Macedonia, With Particular Reference to the Allchar Deposit. Faculty of Mining and Geology, Štip (Special Issue No. 5, 262 pp.).

John, D.M., Whitton, B.A., Brook, A.J., 2002. The Freshwater Algal Flora of the British Isles: An Identification Guide to Freshwater and Terrestrial Algae. Cambridge University Press.

Jordaens, K., De Wolf, H., Vandecasteele, B., Blust, R., Backeljau, T., 2006. Associations between shell strength, shell morphology and heavy metals in the land snail *Cepaea nemoralis* (Gastropoda, Helicidae). Sci. Total Environ. 363, 285–293.

Kaonga, C.C., Chiotha, S.S., Monjerezi, M., Fabiano, E., Henry, E.M., 2008. Levels of cadmium, manganese and lead in water and algae; *Spirogyra aequinoctialis*. Int. J. Environ. Sci. Technol. 5 (4), 471–478.

Karbowska, B., 2016. Presence of thallium in the environment: sources of contaminations, distribution and monitoring methods. Environ. Monit. Assess. 188 (11), 640.

Kelly, M., Juggins, S., Guthrie, R., Pritchard, S., Jamieson, J., Rippey, B., Hirst, H., Yallop, M., 2008. Assessment of ecological status in UK rivers using diatoms. Freshw. Biol. 53, 403–422.

Krammer, K., 2002. Diatoms of Europe Diatoms of the European Inland Waters and Comparable Habitats Vol 3. Cymbella ARG Gantner Verlag KG, Ruggell.

Krammer, K., Lange-Bertalot, H., 1991a. Bacillariophyceae 3 Teil: Centrales, Fragilariaceae, Eunotiaceae. In: Ettl, H., Gerloff, J., Heynig, H., Mollenhauer, D. (Eds.), Süsswasserflora von Mitteleuropa. Band 2/3 Gustav Fischer Verlag, Stuttgart, Jena.

Krammer, K., Lange-Bertalot, H., 1991b. Bacillariophyceae. 4. Teil: Achnanthaceae, Kritische Ergänzungen zu Navicula (Lineolatae) und Gomphonema, Gesamtliteraturverzeichnis Teil 1-4. In: Ettl, H., Gärtner, G., Gerloff, J., Heynig, H., Mollenhauer, D. (Eds.), Süsswasserflora von Mitteleuropa. Band 2/4 Gustav Fischer Verlag, Stuttgart, Jena.

Kumar, J.I., Oommen, C., 2012. Removal of heavy metals by biosorption using freshwater alga *Spirogyra hyaline*. J. Environ. Biol. 33, 27–31.

Lange-Bertalot, H., 2001. Diatoms of Europe - Volume 2: The Genus *Navicula sensu* Stricto 10 Genera Separated From *Navicula sensu* lato. Frustulia. A.R.G. Gantner Verlag Komanditgesellschaft, Ruggell.

Lange-Bertalot, H., Genkal, S.I., 1999. Iconographia Diatomologica: Annotated Diatom Micrographs Volume 6: Phytogeography-Diversity-Taxonomy. Koeltz Scientific Books.

Latimer WM (1952) Oxidation Potential 2nd ed., Prentice Hall Garrels, RM, Christ, LC (1990).

Lau, S., Murtedza, M., Sabtuyah, S., 1996. Heavy metals in sediment as a tracer for sources of pollution in Sg Sarawak. Malays. J. Anal. Sci. 2 (2), 365–371.

Lepitkova, S., Boev, B., Dimevski, V., Boev, I., Eminov, H., Georgiev, L., 2013. Geochemical analysis of a bean seed in certain regions in the Republic of Macedonia. Geol. Macedon. 25 (1), 53–59.

Lin, T.-S., Nriagu, J., 1999. Thallium separation in Great Lakes. Environ. Sci. Technol. 33, 3394–3397.

Maidment, D.R., 1992. Handbook of Hydrology. McGraw-Hill, Inc., New York, NY (608 pp.).

Makovicky, E., Balić Žunić, T., 1993. Contributing to the crystal chemistry of thallium sulphosalts. II. TlSb3Ss-the missing link of the lillanite homologous series. N. Jb. Mineral. (Abh.) 165 (3), 331–344.

Migaszewski, Z.M., Gałuszka, A., Pasławski, P., Starnawska, E., 2007. An influence of pyrite oxidation on generation of unique acidic pit water: a case study, Podwiśniówka Quarry, Holy Cross Mountains (South-Central Poland). Pol. J. Environ. Stud. 16 (3), 407–421.

Mishra, A., Kavita, K., Jha, B., 2011. Characterization of extracellular polymeric substances produced by micro-algae *Dunaliella salina*. Carbohydr. Polym. 83, 852–857.

Musić, S., Ristić, M., 1988. Adsorption of trace elements or radionucleids on hydrous iron oxides. J. Radioanal. Nucl. Chem. 1208 (2), 289–304.

Nelson, S.M., Roline, R.A., 1996. Recovery of a stream macroinvertebrate community from mine drainage disturbance. Hydrobiologia 339, 73–84.

Nordstrom, D.K., Blowes, D.W., Ptacek, C.J., 2015. Hydrogeochemistry and microbiology of mine drainage: an update. Appl. Geochem. 57, 3–16.

Novis, P.M., Harding, J.S., 2007. Extreme acidophiles: fresh water algae associated with acid mine drainage. In: Seckbach, J. (Ed.), Algae and Cyanobacteria in Extreme Environment. Springer, Dordrecht, pp. 443–464.

Patrick, R., Reimer, C.W., 1975. The Diatoms of the United States, Exclusive of Alaska and Hawaii Volume 2 Part 1: Entomoneidaceae, Cymbellaceae, Gomphonemaceae, Epithemiaceae. The Academy of Natural Sciences of Philadelphia.

Pavičević, M.K., Cvetković, V., Niedermann, S., Pejović, V., Amthauer, G., Boev, B., Bosch, F., Aničin, I., Henning, W.F., 2016. Erosion rate study at the Allchar deposit (Macedonia) based on radioactive and stable cosmogenic nuclides ([26]Al, [36]Cl, [3]He, and [21]Ne). Geochem. Geophys. Geosyst. 17, 410–424.

Percival, T., Boev, B., 1990. As-TI-Sb-Hg-Au-Ba mineralization, Allchar District, Yugoslavia; a unique type of Yugoslavian ore deposit. In: Int. Symposium on Solar Neutrino Detection With 205Tl. Yug. Soc. Nucl. Elemen. Pert. Phys, Dubrovnik, pp.

36–37 (Abstract).

Percival, T., Radtke, A., 1994. Sedimentary rock-hosted disseminated gold mineralization in the Allchar District, Macedonia. Can. Mineral. 32, 649–665.

Queirolo, F., Stegen, S., Contreras-Ortega, C., Ostapczuk, P., Queirolo, A., Paredes, B., 2009. Thallium levels and bioaccumulation in environmental samples of northern Chile: human health risks. J. Chil. Chem. Soc. 54 (4), 464–469.

Rajfur, M., Klos, A., Waclawek, M., 2010. Sorption properties of algae *Spirogyra* sp and their use for determination of heavy metal ions concentrations in surface water. Bioelectrochemistry 80, 81–86.

Rajfur, M., Klos, A., Waclawek, M., 2011. Algae utilization in assessment of the large Turawa Lake (Poland) pollution with heavy metals. J. Environ. Sci. Health A 46, 1401–1408.

Rasmussen, K., Lindegaard, C., 1988. Effects of iron compounds on macroinvertebrate communities in a Danish lowland river system. Water Res. 22 (9), 1101–1108.

Robie, R.A., Hemingway, B.S., Fisher, J.R., 1978. Thermodynamic properties of minerals and related substances at 298.15 K and 1 bar (105 Pascals) pressure and at higher temperatures. Bull. US Geol. Surv. 1452.

Rossmässler, E.A., 1835–1837. Iconographie der Land- und Süßwasser-Mollusken, mit vorzüglicher Berücksichtigung der europäischen noch nicht abgebildeten Arten. Erster Band. - pp. Heft 1: [1], I-VI [=1-6], 1-132, [1-2], Heft 2: [1-2], 1-26, Heft 3: [1-3], 1-33, Heft 4: [1-3], 1-27, Heft 5-6: [1-3], 1-70, Taf. 1-30. Dresden, Leipzig. (Arnold).

Rott, E., Pipp, E., Pfister, P., van Dam, H., Ortler, K., Binder, N., Pall, K., 1999. Indikationslisten für Aufwuchsalgen in Österreichischen Fliessgewassern. Teil 2: Trophieindikation. Bundesministerium fuer Land- und Forstwirtschaft, Wien.

Round, F.E., Crawford, R.M., Mann, D.G., 1990. The Diatoms: Biology & Morphology of the Genera. Cambridge University Press.

Salminen, R., Batista, M.J., Bidovec, M., Demetriades, A., De Vivo, B., De Vos, W., Duris, M., Gilucis, A., Gregorauskiene, V., Halamic, J., Heitzmann, P., Lima, A., Jordan, G., Klaver, G., Klein, P., Lis, J., Locutura, J., Marsina, K., Mazreku, A., O'Connor, P.J., Olsson, S.Å., Ottesen, R.T., Petersell, V., Plant, J.A., Reeder, S., Salpeteur, I., Sandström, H., Siewers, U., Steenfelt, A., Tarvainen, T., 2005. FOREGS Geochemical Atlas of Europe, Part 1: Background Information, Methodology and Maps. Geological Survey of Finland, Espoo Available online at: http://www.gtk.fi/publ/foregsatlas/ (526 pp.).

Serafimovski, T., Boev, B., Tasev, G., 2012. Some quantitative aspects of the major types of ores at the Ržanovo Fe-Ni lateritic deposit, R. Macedonia. Geol. Macedon. 26 (1), 21–35.

Stafilov, T., Todorovski, T., 1987. Determination of gold in arsenic-antimony ore by flame-less atomic absorption spectrometry. J. At. Spectrom. 8, 12–14.

Stevenson, R.J., Pan, Y., 1999. Assessing environmental conditions in rivers and streams with diatoms. In: The Diatoms: Applications for the Environmental and Earth Sciences. Cambridge University Press, Cambridge, pp. 11–40.

Strmić Palinkaš, S., Hofstra, A.H., Percival, T.J., Borojević Šoštarić, S., Palinkaš, L., Bermanec, V., Pecskay, Z., Boev, B., 2018. Comparison of the Allchar Au-As-Sb-Tl Deposit, Republic of Macedonia With Carlin-type Gold Deposits. (in press).

Szekeres, M., Tombácz, E., 2012. Surface charge characterization of metal oxides by potentiometric acid-base titration, revisited theory and experiment. Colloids Surf. A

Physicochem. Eng. Asp. 414, 302–313.

Tallman, D.E., Shaikh, A.U., 1980. Redox stability of inorganic arsenic(III) and arsenic(V) in aqueous solution. Anal. Chem. 52, 196–199.

Talukdar, B., Basumatary, S., Kalita, H.K., Baishya, R.A., Dutta, A., Srivastava, S.K., Sarma, D., 2015. Histopathological alternations in liver and kidney of Tor tor (Ham) inhabited in coal mining affected areas of Simsang River, Garohills; Meghalaya. Natl. Acad. Sci. Lett. 38 (4), 321–324.

Talukdar, B., Kalita, H.K., Basumatary, S., Saikia, D.J., Sarma, D., 2017. Cytotoxic and genotoxic effects of acid mine drainage on fish *Channa punctata* (Bloch). Ecotoxicol. Environ. Saf. https://doi.org/10.1016/j.ecoenv.2017.06.007.

Tingzong, G., DeLaune, R.D., Patrick Jr., W.H., 1997. The influence of sediment redox chemistry on chemically active forms of arsenic, cadmium, chromium, and zinc in estuarine sediment. Environ. Int. 23 (3), 305–316.

Tremaine, P.R., LeBlanc, J.C., 1980. The solubility of magnetite and the hydrolysis and oxidation of Fe^{2+} in water to 300 °C. J. Solut. Chem. 9, 415. https://doi.org/10.1007/BF00645517.

Tremel, A., Masson, P., Sterckeman, T., Baize, D., Mench, M., 1997. Thallium in French agrosystems: I-thallium contents in arable soils. Environ. Pollut. 95 (3), 293–302.

Vetrivel, S.A., Diptanghu, M., Ebhin, M.R., Sydavalli, S., Gaurav, N., Tiger, K.P., 2017. Green algae of the genus *Spirogyra*: a potential absorbent for heavy metal from coal mine water. Remediation. https://doi.org/10.1002/rem.21522.

Vogel, M., Gunther, A., Rossberg, A., Li, B., Bernhard, G., Raff, J., 2010. Biosorption of U (VI) by the green algae *Chlorella vulgaris* in dependence of pH value and cell activity. Sci. Total Environ. 409, 384–395.

Wagman, D.D., Evans, W.H., Parker, V.B., Halow, I., Bailey, S.M., Schumm, R.H., 1968. Selected values of chemical thermodynamic properties. In: NBS Technical Note 270-3.

Wagman, D.D., Evans, W.H., Parker, V.B., Halow, I., Bailey, S.M., Schumm, R.H., 1969. Selected values of chemical thermodynamic properties. In: NBS Technical Note 270-4.

Wagman, D.D., Evans, W.H., Parker, V.B., Schumm, R.H., Halow, I., Bailey, S.M., Churney, K.L., Nuttal, R.L., 1982. The NBS tables of chemical thermodynamic properties. Selected values for inorganic and C1 and C2 organic substances in SI units. J. Phys. Chem. Ref. Data 11 (supplement 2) (392 pp., In: Robie RA and Hemingway BS (1995) Thermodynamic properties of minerals and related substances at 290.15 K and one bar (10 5 pascals) pressure and at high temperatures. US Geol Surv Bull 1452).

Wegl, R., 1983. Index für die Limnosaprobitaet -Wasser und Abwasser Beitraege zur Gewaesserforschung. 26. pp. 1–175.

Wehr, J.D., Sheath, R.G., 2003. Freshwater Algae of North America. Ecology and Classification Academic Press.

Wilcock, J.R., Perry, C.C., Williams, R.J.P., Brook, A.J., 1989. Biological minerals formed from strontium and barium sulphates. II. Crystallography and control of mineral morphology in desmids. Proc. R. Soc. Lond. Ser. B 238 (1292), 203–221.

Winterbourn, M.J., McDiffett, W.F., Eppley, S.J., 2000. Aluminium and iron burdens of aquatic biota in Zealand streams contaminated by acid mine drainage: effects of trophic level. Sci. Total Environ. 254, 45–54.